

1 **Bias correction schemes for CMORPH satellite rainfall**
2 **estimates in the Zambezi River Basin**

3 **W. Gumindoga^{ab}, T.H.M. Rientjes^a, A.T. Haile^c, H. Makurira^b and P. Reggiani^d**

4 *^aFaculty ITC, University of Twente, The Netherlands*

5 *^bUniversity of Zimbabwe, Civil Eng. Department Box MP 167 Mt Pleasant, Harare, Zimbabwe*

6 *^cInternational Water Management Institute (IWMI), Ethiopia*

7 *^dUniversity of Siegen, Germany*

8

9 *Email of corresponding author: w.gumindoga@utwente.nl OR wgumindoga@gmail.com*
10

11

12

13

14 First submission: 27 January 2016

15

16

17

18

19 *Email of corresponding author: w.gumindoga@utwente.nl*

20

21

22

23

24 **Abstract**

25 Obtaining reliable records of rainfall from satellite rainfall estimates (SREs) is a challenge as
26 SREs are an indirect rainfall estimate from visible, infrared (IR), and/or microwave (MW)
27 based information of cloud properties. SREs also contain inherent biases which exaggerate or
28 underestimate actual rainfall values hence the need to apply bias correction methods to improve
29 accuracies. We evaluate the performance of five bias correction schemes for CMORPH
30 satellite-based rainfall estimates. We use 54 raingauge stations in the Zambezi Basin for the
31 period 1998–2013 for comparison and correction. Analysis shows that SREs better match to

32 gauged estimates in the Upper Zambezi Basin than the Lower and Middle Zambezi basins but
33 performance is not clearly related to elevation. Findings indicate that rainfall in the Upper
34 Zambezi Basin is best estimated by an additive bias correction scheme (Distribution
35 transformation). The linear based (Spatio-temporal) bias correction scheme successfully
36 corrected the daily mean of CMORPH estimates for 70 % of the stations and also was most
37 effective in reducing the rainfall bias. The nonlinear bias correction schemes (Power transform
38 and the Quantile based empirical-statistical error correction method) proved most effective in
39 reproducing the rainfall totals. Analyses through bias correction indicate that bias of CMORPH
40 estimates has elevation and seasonality tendencies across the Zambezi river basin area of large
41 scale.

42

43 **Keywords:** *Bias correction factor, Seasonality influences, Space-time variable, Elevation*
44 *influences*

45

46 **1. Introduction**

47 A plethora of error (hereafter bias) correction schemes for satellite-derived rainfall estimates
48 (SREs) have been published (e.g. Woody et al., 2014; Habib et al., 2014; Vernimmen et al.,
49 2012; Gebregiorgis et al., 2012; Tesfagiorgis et al., 2011; Shrestha, 2011). Bias correction
50 schemes are important because SREs are prone to systematic and random errors related to the
51 fact that SREs are indirect rainfall estimates from visible, infrared (IR), and/or microwave
52 (MW) based information of cloud properties (Pereira Filho et al., 2010). Bias is defined as the
53 systematic error or difference between raingauge estimates and SREs, and can be positive or
54 negative (Moazami et al., 2013; Qin et al., 2014). Bias can be expressed for rainfall depth, its
55 occurrence and intensity. Bias often exhibit a topographical and latitudinal dependency as, for
56 instance, shown for the National Oceanic and Atmospheric Administration (NOAA) Climate
57 Prediction Center-MORPHing (CMORPH) bias in the Nile Basin (Bitew et al., 2011; Habib et
58 al., 2012; Haile et al., 2013). For Southern Africa, Dinku et al (2008) and Thorne et al (2001)
59 show that bias in rainfall occurrences and intensities can be related to location, topography,
60 local climate and season. SRE's tested are Tropical Applications of Meteorological Satellites
61 (TAMSAT), Tropical Rainfall Measuring Mission (TRMM-3B42), Precipitation Estimation
62 from Remotely Sensed Information using Artificial Neural Network (PERSIANN) and Climate
63 Hazards Group InfraRed Precipitation with stations (CHIRPS). Studies in the Zambezi Basin,
64 show evidence necessitating the correction of bias in SREs by comparing SREs against gauge
65 observations. For example Cohen Liechti (2012) show that CMORPH rainfall have challenges
66 in estimation of rainfall volumes at daily and monthly scales. Matos et al. (2013) and Thiemi
67 et al. (2012) show that bias varies across geographical domains in the basin and may be as large
68 as $\pm 50\%$. Negative bias indicates underestimation of rainfall whereas positive bias indicates
69 overestimation (Moazami et al., 2013).

70

71 Bias correction schemes serve to correct for systematic errors of the SREs and aim to improve
72 the reliability of SREs (Tefagiorgis et al., 2011). Most bias correction schemes rely on
73 assumptions that adjust for rainfall variability in space and time (Habib et al., 2014). As such,
74 methodologies for bias correction were developed for multi-sensor (Breidenbach and
75 Bradberry, 2001) and radar-gauge approaches (Vernimmen et al., 2012), and for climate
76 models (Lafon et al., 2013) that provide rainfall estimates systematically in the time domain
77 covering vast areas. Examples of correction schemes are mean bias (Seo et al., 1999), ratio bias
78 (Anagnostou et al., 1999;Tefagiorgis et al., 2011), distribution transformation (Bouwer,
79 2004), spatial bias (Bajracharya et al., 2014), histogram equalisation (Thiemig et al., 2013),
80 regression analysis (Cheema and Bastiaanssen, 2010;Shrestha, 2011;Yin et al., 2008) and
81 probability distribution function (QME) matching (Gudmundsson et al., 2012;Gutjahr and
82 Heinemann, 2013).

83
84 Most bias correction schemes have background in climate models. Schemes aim to correct bias
85 for satellite precipitation totals but do not address aspects of temporal variability of the
86 precipitation (Botter et al., 2007). Bias correction techniques such as those based on regression
87 techniques where rainfall totals are corrected relative to estimates from a reference rain gauge
88 station, have reported distortion of frequency and intensity of rainfall (Botter et al., 2007). On
89 one hand, some bias schemes are developed using multiplicative shifts procedures and tend to
90 adjust only rainfall intensity to reproduce the long-term mean observed monthly rainfall, but
91 these are reported not to correct any systematic error in rainfall frequency ~~rainfall~~ (Ines and
92 Hansen, 2006). On the other hand, non-multiplicative bias correction procedures provide an
93 option for using the daily corrected satellite rainfall in a manner that preserves any useful
94 information about the timing of rainfall ~~frequency~~ within a season (Fang et al., 2015;Hempel
95 et al., 2013). For many hydrologic applications correct representation of daily rainfall is
96 important. Non-linear bias correction schemes are well known in literature for mitigating the
97 underestimation of SREs in dry months without leading to an overestimation of rainfall during
98 wet months (Vernimmen et al., 2012). Power function derived bias correction schemes correct
99 for extreme values (depth, intensity, rate and occurrence) in CMORPH estimates (Vernimmen
100 et al., 2012). Contrary, the Bayesian (likelihood) analysis techniques are found to over-adjust
101 both light and strong rainfall intensities toward more intermediate intensities (Tian et al., 2010).

102
103 Besides that bias may change over time, some correction schemes (e.g. the γ -distribution
104 correction method) do not account for spatial patterns in bias (Müller and Thompson, 2013).
105 Studies by Habib et al. (2014) and Tefagiorgis et al. (2011) evaluated different forms of the
106 space bias correction schemes. They concluded that the space fixed (invariant) technique which
107 is obtained by using gauge and or SREs bias values lumped over the entire domain is ineffective
108 in reducing rainfall bias as compared to space variant technique. This approach of using the
109 average bias for all stations (space fixed) to correct SREs has its roots in radar rainfall (Seo et

110 al., 1999) and is unsuitable in large basins ($> 10,000 \text{ km}^2$) where bias varies spatially and over
111 time (see Habib et al., 2012).

112

113 Applications of bias correction schemes mostly are reported for northern America, Europe and
114 Australia. For less developed areas such as in the Zambezi Basin (Southern Africa) that is
115 selected for this study applications are very limited. This is despite the strategic importance of
116 the basin in providing water to over 50 million people. An exception is the correction of the
117 TRMM-3B42 product for agricultural purposes in the Upper Zambezi Basin (Beyer et al.,
118 2014). Previous studies on use of SREs in the Zambezi river basin mainly focused on accuracy
119 assessment of SREs with standard statistical indicators with little or no effort to perform bias
120 correction despite the evidence of errors in these products. The use of uncorrected satellite
121 rainfall is reported for hydrological modelling in the Nile Basin (Bitew and Gebremichael,
122 2011) and Zambezi Basin (Cohen Liechti et al., 2012), respectively, and for drought monitoring
123 in Mozambique (Toté et al., 2015). Our selection of CMORPH satellite rainfall for this study
124 is based on the fact that the product has successful applications in African basins such as in
125 hydrological modelling (Habib et al., 2014) and flood predictions in West Africa (Thiemig et
126 al., 2013).

127

128 The objective of this study is to assess suitability of bias correction of CMORPH satellite
129 rainfall estimates in the Zambezi River Basin for the period 1998-2013 for which time series
130 are available from 54 rain gauge stations. Specific objectives are 1) to perform quality control
131 on gauge based estimates in the Zambezi Basin 2) to develop linear/non-linear and time-space
132 variant/invariant bias correction schemes using gauge based estimates in the basin 3) to apply
133 and compare bias correction schemes to CMORPH satellite rainfall and 4) To assess the
134 influence of elevation and seasonality on CMORPH performance and bias correction in the
135 basin.

136

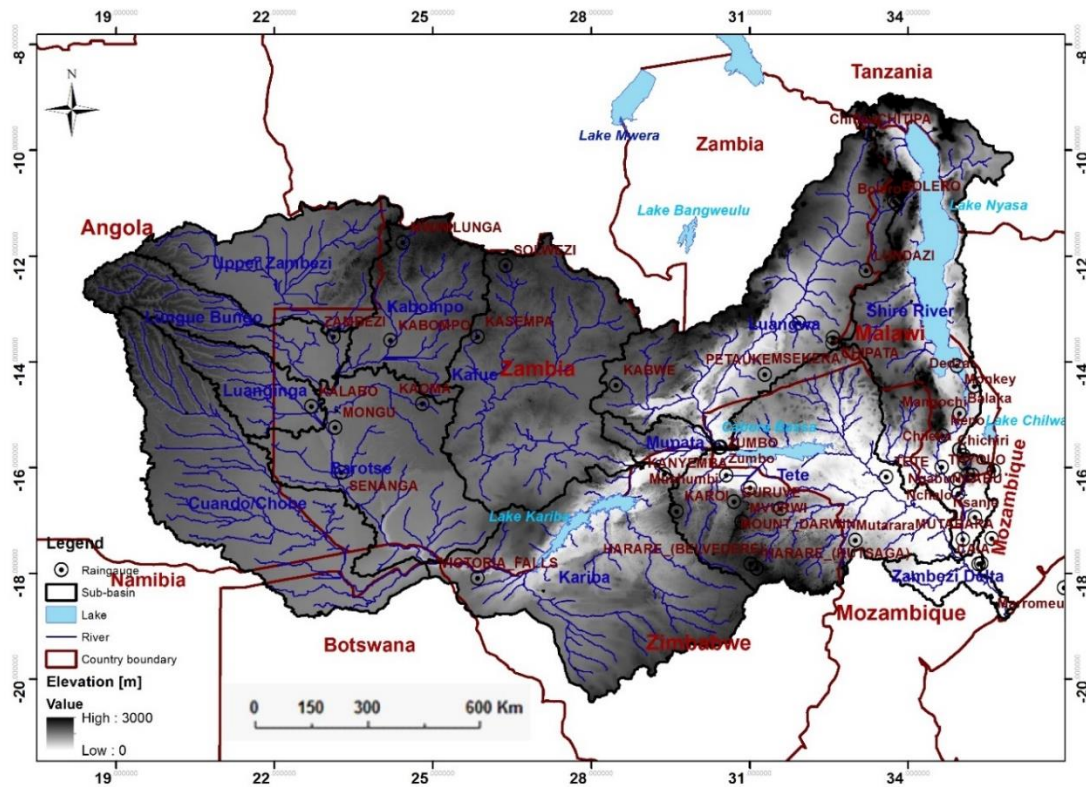
137 This article is organised as follows: Section 2 gives a description of the study area and data
138 availability. Methods used in this study are described in Section 3. Findings of the study are
139 presented in Section 4. Section 5 concludes and discusses findings of the study.

140

141 **2. Study area**

142 The Zambezi River is the fourth-longest river (~2,574 km) in Africa and basin area of
143 ~1,390,000 km^2 (~4 % of the African continent). The river drains into the Indian Ocean and
144 has mean annual discharge of 4,134 m^3/s (World Bank, 2010b). The river has its source in
145 Zambia and partly constitutes boundaries of Angola, Namibia Botswana, Zambia, Zimbabwe
146 and Mozambique (Fig. 1). Because of its vastness in size, the basin has much difference in
147 elevation, topography and climatic seasonality. For that reason the basin well suited for this
148 study and divided into three hydrological regions, i.e., the lower Zambezi comprising the Tete,
149 Lake Malawi/Shire, and Zambezi Delta subbasins, the middle Zambezi made up of the Kariba,

150 Mupata, Kafue, and Luangwa sub catchments, and the Upper Zambezi constituted by the
 151 Kabompo, Lungwebungo, Luanginga, Barotse, and Cuando/Chobe subbasins (Beilfuss, 2012).
 152



153
 154 **Figure 1: Zambezi River Basin with sub basins, major lakes, rivers, elevation and locations of the 54 rain gauging stations**
 155 **used in this study.**

156
 157 The elevation of the Zambezi basin ranges from 0.0 m (for some parts of Mozambique) to
 158 ~3000 m above sea level (for some parts of Zambia). Typical landcover types are woodland,
 159 grassland, water surfaces and cropland (Beilfuss et al., 2000). The basin is characterized by
 160 high annual rainfall (>1,400 mm) in the northern and north-eastern areas but low annual rainfall
 161 (<500 mm) in the southern and western parts (World Bank, 2010a). Due to the varied rainfall
 162 distribution, northern tributaries contribute much more water to the Zambezi River (e.g., the
 163 Upper Zambezi Basin contributes 60 % of total discharge) (Tumbare, 2000). The River and its
 164 tributaries are subject to **cycles of floods and droughts** that have devastating effects on the
 165 people and economies of the region, especially the poorest members of the population
 166 (Tumbare, 2005). It is not uncommon to experience both floods and droughts within the same
 167 hydrological year.

168
 169 **3. Materials and Methodology**

170
 171 **3.1. Data**

172
 173 **3.1.1. Satellite derived rainfall**

174 For this study time series (1998-2013) of CMORPH rainfall product at (8 km × 8 km, 30
175 minutes resolution are selected. Images were downloaded from the GeoNETCAST ISOD
176 toolbox by means of ILWIS GIS software (<http://52north.org/downloads/>). CMORPH
177 estimates are derived from a combination of infrared (IR) temperature fields from geostationary
178 satellites and passive microwave (PMW) temperature fields from polar orbiting satellites at 30
179 minute temporal resolution (Joyce et al., 2004). For this study, data were aggregated to daily
180 totals to match the observation interval from available gauge measurements.

181

182 3.1.2. Gauge based rainfall data

183 Time series of daily rainfall from 60 stations was obtained from meteorological departments
184 Mozambique, Malawi, Zimbabwe and Zambia that cover the study area. After screening, 6
185 stations with suspicious rainfall values were removed from the analysis to remain with 54
186 stations. Although a number of the 54 stations are affected by data gaps, the available time
187 series are of sufficiently long duration (Table 1) to serve objectives of this study. The locations
188 of the stations cover a wide range of elevation values (3 m to 1600 m amsl.) allowing to assess
189 the effect of elevation on the SREs.

190

191 Table 1: HERE

192

193 3.1.3. Gauge based analysis: elevation influences

194

195 To investigate elevation influence on CMOPRH performance, the hierarchical cluster ‘within-
196 groups linkage’ method in SPSS software was used to classify the Zambezi Basin into 3
197 elevation zones (Table 2). This was based on elevation vs correlation coefficient of CMORPH
198 and gauge based estimates. The Advanced Spaceborne Thermal Emission and Reflection
199 Radiometer (ASTER) based 30m DEM obtained from <http://gdem.ersdac.jspacesystems.or.jp/>,
200 was used to represent elevation across the Zambezi basin.

201

202 Table 2: HERE

203

204 Figure 2 shows Mean Annual Rainfall (MAR) isohyets by inverse distance interpolation of
205 mean annual gauged measurements (1998-2013).

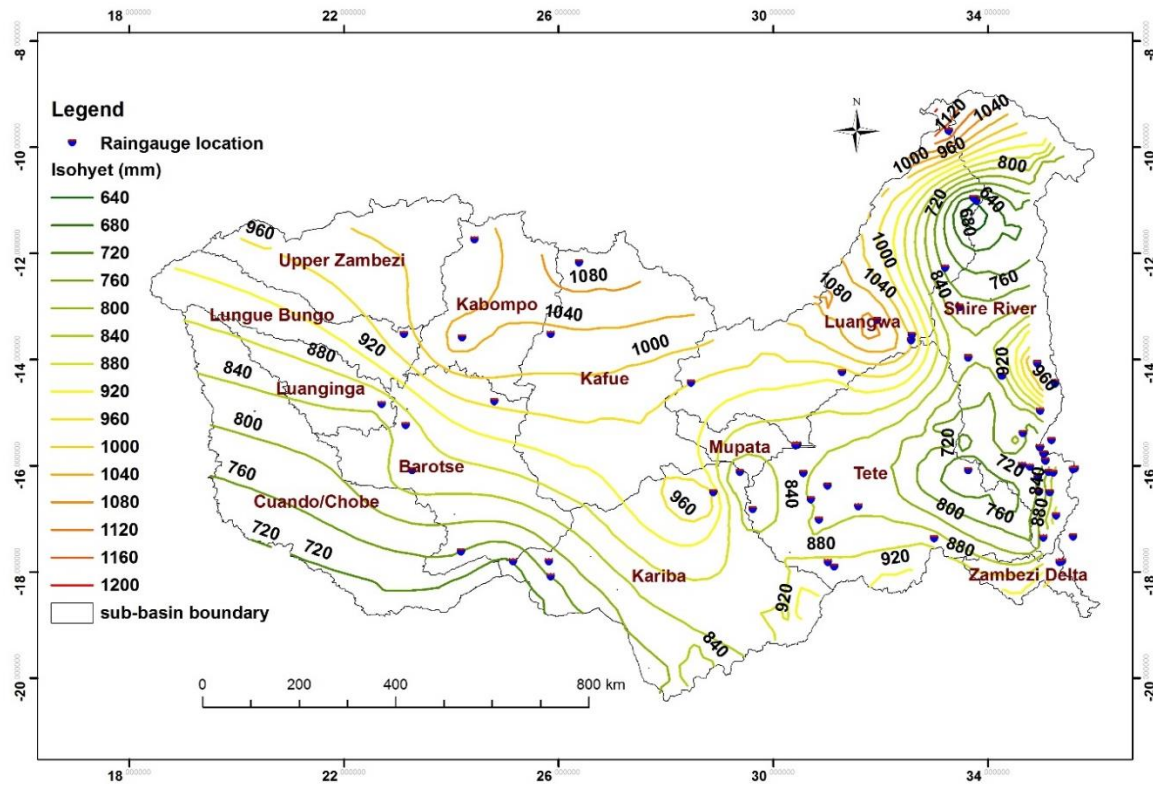


Figure 2: Mean Annual Rainfall (MAR) distribution for the Zambezi Basin (1998-2013).

The double mass-curve was used to check the consistency of rainfall of a single station with poor correlation coefficient (<0.4) against rainfall of nearby other stations (within 100 km radius) in the study area, following Searcy and Hardson (1960). Inconsistencies shown in the double mass-curve may be due to errors in the raingauge data collection. Any unreliable and inconsistent daily rainfall estimate for any year may be adjusted following:

$$P_a = \frac{b_a}{b_o} P_o \quad [1]$$

Where:

- P_a = adjusted rainfall station X in any year
- P_o = observed rainfall for station X in the same year
- b_a = slope of graph to which records are adjusted
- b_o = slope of graph at time P_o was observed

3.2. Bias correction schemes

In this study, the bias in CMORPH rainfall estimates was assessed and corrected using 5 schemes. Based on preliminary analysis on rainfall distributions in the Zambezi Basin, the bias correction factor is calculated for a certain day only when a minimum of five rainy days were recorded within the preceding ten-day window with a minimum rainfall accumulation depth of 5 mm, otherwise no bias is estimated (i.e. a value of 1 is assigned). This means bias factors change value for each station for each 10 day period.

230

231 3.2.1. Spatio-temporal bias correction (STB)

232 This linear bias correction scheme has its origin in the correction of radar based precipitation
233 estimates (Tefagiorgis et al., 2011) and downscaled precipitation products from climate
234 models (Lenderink et al., 2007;Teutschbein and Seibert, 2013). The bias is corrected for
235 individual raingauge stations at daily time step implying that bias correction varies in space and
236 over time, and is based on the use of the BF_{STB} factor estimated from equation [2]:

237

$$238 \quad BF_{STB} = \frac{\sum_{t=d-l}^{t=d-1} S(i,t)}{\sum_{t=d-l}^{t=d-1} G(i,t)} \quad [2]$$

239 The CMOPRH daily rainfall estimates are then multiplied by the BF_{STB} for the respective time
240 windows resulting in corrected CMORPH estimates in a temporally and spatially coherent
241 manner. The advantages of the bias scheme are the simplicity and modest data requirements
242 and that it adjusts the daily mean of CMORPH at each station.

243

244 Where:

245	G and S	=	daily gauge and CMORPH rainfall estimates, respectively
246	i	=	gauge location
247	t	=	julian day number
248	l	=	length of a time window for bias calculation
249	n	=	the total number of gauges within the entire domain of the study
250	T	=	full duration of the study period.

251

252 3.2.2. Elevation zone bias correction (EZB).

253 This bias scheme is proposed in this study and aims at correction of satellite rainfall by
254 understanding elevation influences on the rainfall distribution. The method groups raingauge
255 stations into 3 elevation zones (Table 2). The assumption is that stations in the same elevation
256 zone have the same error characteristics and are assigned a spatial but temporally variant bias
257 correction factor. The resulting bias correction factor is used to adjust satellite estimates by
258 multiplying each daily station data by the daily bias factor, BF_{EZB} .

259

$$260 \quad BF_{EZB} = \frac{\sum_{t=d-l}^{t=d-1} \sum_{i=1}^{i=n} S(i,t)}{\sum_{t=d-l}^{t=d-1} \sum_{i=1}^{i=n} G(i,t)} \quad [3]$$

261 The merits of this bias correction scheme is that the daily time variability is preserved up to a
262 constant multiplicative factor and at the same time accounting for spatial heterogeneity in
263 topography (but fixed for each zone).

264

265 3.2.3. Power transform (PT)

266 This nonlinear bias correction scheme is aimed at achieving a closer fit between monthly
 267 CMORPH and raingauge data. The bias scheme has its origins in general circulation models
 268 (Lafon et al., 2013) but has been extended to satellite rainfall estimates for hydrological
 269 modelling and drought monitoring (Vernimmen et al., 2012). The bias corrected CMORPH
 270 rainfall (P^*) is obtained using:

$$271 \quad P^* = aP^b \quad [4]$$

272 Where

273 P = raingauge monthly rainfall

274 a = prefactor such that the mean of the transformed precipitation values is equal to the
 275 gauge based mean.

276 b = factor calculated iteratively such that for each station the Coefficient of Variation
 277 (CV) of CMORPH matches the gauge based estimates
 278

279
 280 Optimized values of a and b are obtained through the generalized reduced gradient algorithm
 281 (Fylstra et al., 1998). The bias correction is estimated for monthly periods but is applied at daily
 282 time step. The advantage of this bias scheme is that rainfall variability of the daily time series
 283 is preserved by adjusting both the monthly mean and standard deviation of the CMORPH
 284 estimates. The bias scheme also adjusts extreme precipitation values in CMORPH estimates
 285 (Vernimmen et al., 2012).
 286

287 3.2.4. Distribution transformation (DT)

288 This additive approach to bias correction has its origin in statistical downscaling of climate
 289 model data (Bouwer et al., 2004). In this study the method determines the statistical distribution
 290 function at daily base of all raingauge station estimates as well as CMORPH values at the
 291 respective stations. The CMORPH statistical distribution function is matched from the
 292 raingauge data distribution following steps described in equations [5-9]. Both the difference in
 293 mean value and the difference in variation are corrected. First the bias correction factor for the
 294 mean (DT_μ) is determined using equation [5]:

$$295 \quad DT_\mu = \frac{G_\mu}{S_\mu} \quad [5]$$

296 G_μ and S_μ are mean monthly gauge and CMORPH rainfall estimates for all stations,
 297 respectively.
 298

299
 300 Secondly, the correction factor for the variation (DT_τ) is determined by the quotient of the
 301 standard deviations, G_t and S_t , for gauge and CMORPH respectively.

$$302 \quad DT_\tau = \frac{G_\tau}{S_\tau} \quad [6]$$

304 Once the correction factors are established, they are applied to correct all rain gauge stations
 305 data from CMORPH image following:

$$306 \quad S_{DT} = (S_o - S_u)_{DT_r} + DT_\mu * S_r \quad [7]$$

308 Where:

$$309 \quad S_{DT} = \text{corrected CMORPH}$$

$$310 \quad S_o = \text{uncorrected CMORPH}$$

311 The merit of this bias scheme is that it corrects for frequency-based indices such as standard
 312 deviation and percentile values (Fang et al., 2015).

313

314 3.2.5. Quantile mapping based on an empirical distribution (QME)

315 This is a quantile based empirical-statistical error correction method with its origin in empirical
 316 transformation and bias correction of regional climate model-simulated precipitation (Thiemeßl
 317 et al., 2012). The method corrects CMORPH precipitation based on point-wise daily
 318 constructed empirical cumulative distribution functions (ecdfs). The frequency of precipitation
 319 occurrence is corrected at the same time (Thiemeßl et al., 2010).

320

321 The adjustment of precipitation using quantile mapping can be expressed in terms of the
 322 empirical CDF (ecdf) and its inverse (ecdf⁻¹):

$$323 \quad P_{QME} = ecdf_{obs}^{-1}(ecdf_{raw}(P_{raw})) \quad [8]$$

325

326 Where:

$$327 \quad P_{QME} = \text{bias corrected CMORPH}$$

$$328 \quad P_{raw} = \text{uncorrected CMORPH}$$

329

330 The advantage of this bias scheme is that it corrects bias in the mean, standard deviation (Fang
 331 et al., 2015) as well as errors in rainfall depth, The approach is important for long term water
 332 resources assessments under the influence of landuse or climate change. Furthermore, it
 333 preserves the extreme precipitation values (Thiemeßl et al., 2012).

334

335 3.3. Performance evaluation of CMORPH rainfall types

336 A comparison of corrected and uncorrected CMORPH satellite rainfall estimates with rain
 337 gauge data was performed using statistics that measure systematic differences (i.e. bias and
 338 relative bias), accumulated error (e.g. root mean square error), measures of association (e.g.
 339 correlation coefficient) and random differences (e.g. standard deviation of differences and
 340 coefficient of variation) (Haile et al., 2013). Comparison is also made for the dry and wet
 341 seasons and for different rainfall intensities (light rains-heavy rains). The root mean square
 342 error (RMSE), was used to measure the average error following Jiang et al. (2012). Thus RMSE

343 is used to test the accuracy of CMOPRH rainfall estimates against rain gauge based estimates.
 344 The correlation coefficient (CC) was used to assess the agreement between satellite-based
 345 rainfall and rain gauge observations. Equations [9-12] apply.

$$346 \text{Bias} = \frac{\sum(P_{\text{satellite}} - P_{\text{rain gauge}})}{N} \quad [9]$$

$$347 \text{Rbias} = \frac{\sum(P_{\text{satellite}} - P_{\text{rain gauge}})}{\sum P_{\text{rain gauge}}} \quad [10]$$

$$348 \text{RMSE} = \sqrt{\frac{\sum(P_{\text{satellite}} - P_{\text{rain gauge}})^2}{N}} \quad [11]$$

$$349 \text{CC} = \frac{\sum(P_{\text{rain gauge}} - \bar{P}_{\text{rain gauge}})(P_{\text{satellite}} - \bar{P}_{\text{satellite}})}{\sqrt{\sum(P_{\text{rain gauge}} - \bar{P}_{\text{rain gauge}})^2} \sqrt{\sum(P_{\text{satellite}} - \bar{P}_{\text{satellite}})^2}} \quad [12]$$

350
 351
 352 where:

- 353 $P_{\text{satellite}}$ = rainfall estimates by satellite (mm/day)
 354 $\bar{P}_{\text{satellite}}$ = mean values of the satellite rainfall estimates (mm/day)
 355 $P_{\text{rain gauge}}$ = rainfall recorded by rain gauge (mm/day)
 356 $\bar{P}_{\text{rain gauge}}$ = mean values of the rain gauge observations (mm/day)
 357 N = sample size (days).

358 Bias, Rbias and RMSE range from 0.00 (CMORPH measurements = gauge based
 359 measurements) to infinity (CMORPH measurements \neq gauge based measurements) (Mashingia
 360 et al., 2014). Correlation Coefficient (CC) ranges from -1 to 1 with a perfect score of 1.

361
 362 Visual comparison was also done using Taylor diagrams which provides a concise statistical
 363 summary of how well patterns match each other in terms of their CC, their root-mean-square
 364 difference ($RMSE^i$), and the ratio of their variances on a 2-D plot (Taylor, 2001). The reason
 365 that each point in the two-dimensional space of the Taylor diagram can represent the above
 366 three different statistics simultaneously is that root-mean-square difference, and the ratio of
 367 their variances are related by the following:

$$368 \text{RMSE}^i = \delta_f^2 + \delta_r^2 - 2\delta_f\delta_r\text{CC} \quad [13]$$

369 Where:
 370 $\delta_f^2 + \delta_r^2$ = standard deviation between CMORPH and rain gauge rainfall, respectively

371
 372

373 4. Results and Discussion

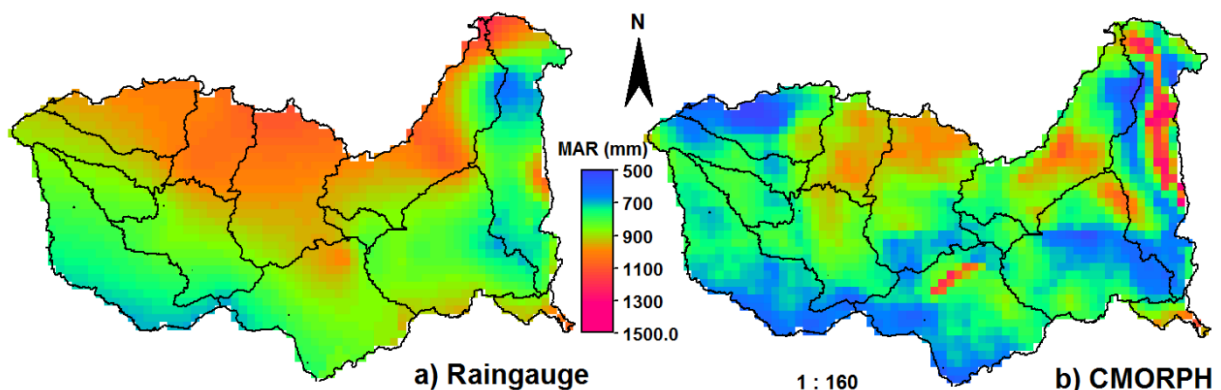
374 4.1. Basic statistics for the CMORPH and gauge estimates

382 The mean rainfall, highest rainfall and sum of the gauged and CMORPH rainfall estimates for
 383 the period 1998-2013 vary widely (Table 3). Statistical scores (based on the mean, maximum
 384 and sum) indicate underestimation of the CMORPH rainfall for both the lowland and the
 385 highland stations, with more underestimation experienced in the highland stations. In as much
 386 CMORPH matches the standard deviation of gauge based estimates (± 2 mm/day) for 30 out
 387 of 54 stations, a summary for the lowland and highland stations shows lower standard deviation
 388 for CMORPH than the gauge based estimates. There are also instances where CMORPH shows
 389 agreement with the gauge estimates (e.g. CV of 3.12 for both CMORPH and gauge in the
 390 highland stations). The minimum recorded rainfall for both the CMORPH and gauge estimates
 391 is 0.0.

392
 393 Table 3: HERE
 394
 395

396 Figure 3 also shows a comparison of the mean annual rainfall (MAR) for the gauge based
 397 estimates (through Universal Krigging interpolation technique) and CMORPH observations in
 398 the Zambezi Basin. The rain gauge map shows higher estimated values in the northern parts of
 399 the basin compared to the CMORPH estimates. There are also patches of higher MAR values
 400 found in the Shire and Kariba Basin for the CMORPH estimates.

401

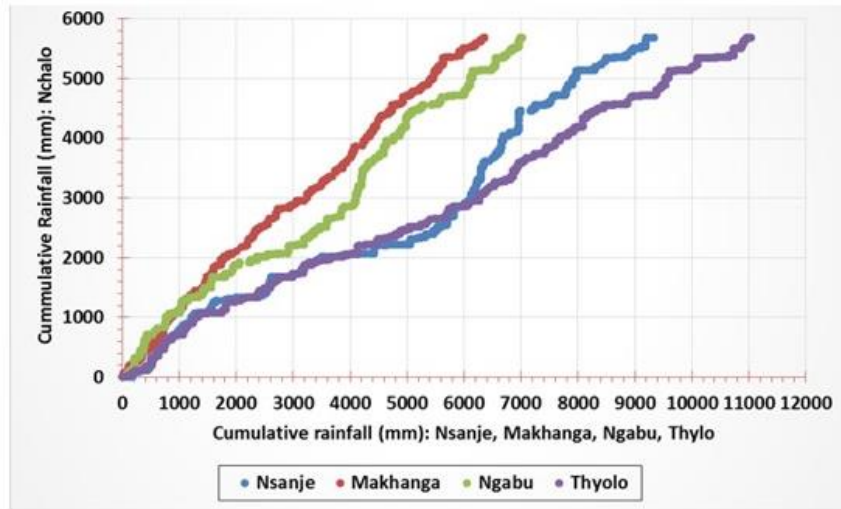


402
 403 **Figure 3: Mean annual rainfall (1998-2013) for the Rain gauge and CMORPH observations in the Zambezi Basin**
 404

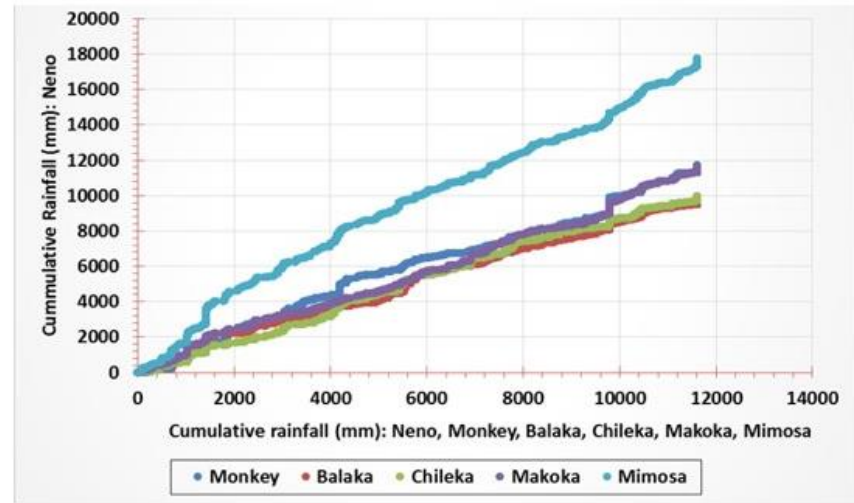
405 4.2. Quality assessment using double-mass curves

406 Figure 4 reports four (4) selected double mass curves, with Figure 4d being the best in terms
 407 of the rainfall matching, followed by Figure 4b and Figure 4c. The worst in terms of match is
 408 Figure 4a. Pairs of stations with less pronounced differences in slope gradients are Neno vs
 409 Monkey, Bolero vs Chitipa and Mvurwi vs Karoi. However, there are stations that show clear
 410 break points and pronounced differences in slope gradients (staircase-like features) in double-
 411 mass curves. These are observed in the Nchalo vs Nsanje, Mvurwi vs Muzarabani and these
 412 could be caused by changes due to errors in the rain gauge data collection at Nchalo or Mvurwi
 413 stations. Results also confirm that stations with relatively greater distance from each other (e.g.
 414 Bolero to Lundazi ~ 180km) shows poor match and hence more pronounced differences in

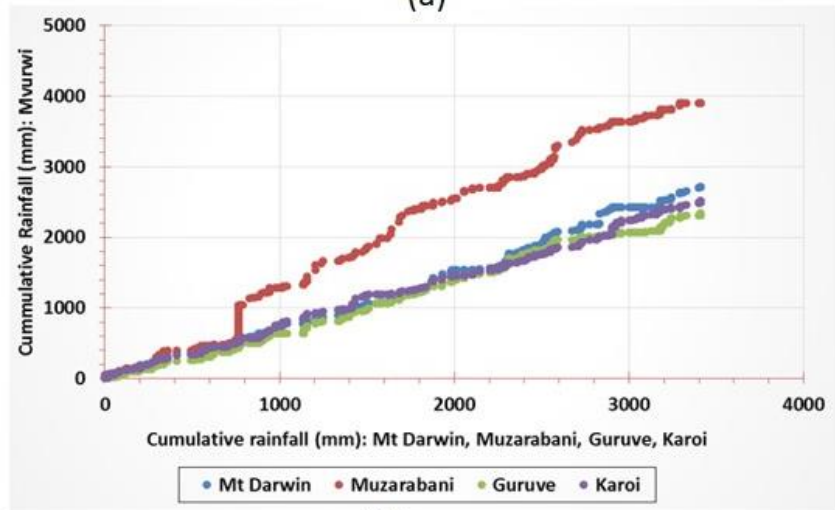
415 slope gradients than stations that have close proximity (e.g. Mvurwi to Guruve ~ 45 km). In
416 addition stations that show close match exhibit similar elevation (e.g. Neno and Makoka have
417 elevation difference ~ 96 m asl.) compared to stations that show poor match (e.g Mvurwi and
418 Muzarabani ~1064 m asl.). In cases where break point are not clearly shown, we used nearby
419 stations to adjust for the inconsistencies in these suspicious stations for years prior to the break.
420 This analysis highlights the critical need for quality gauge based stations that can provide
421 reliable validation datasets as a prerequisite for the assessment of satellite based rainfall
422 estimates and bias correction.



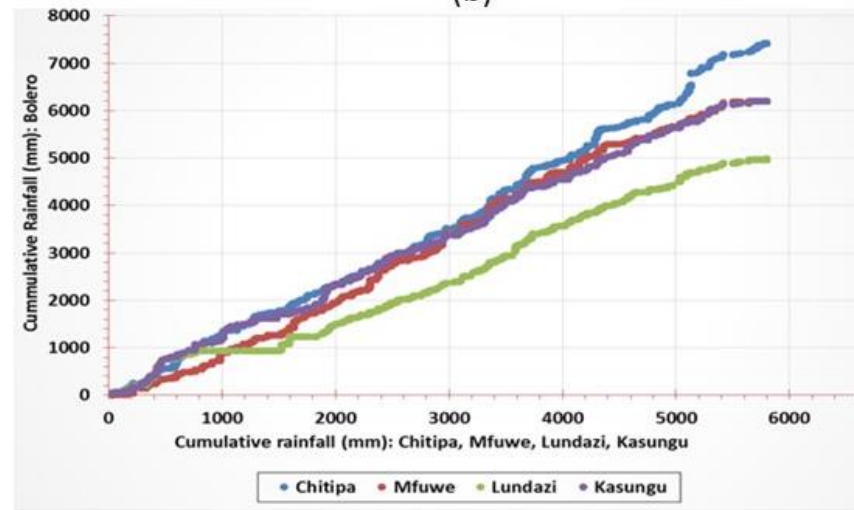
(a)



(b)



(c)



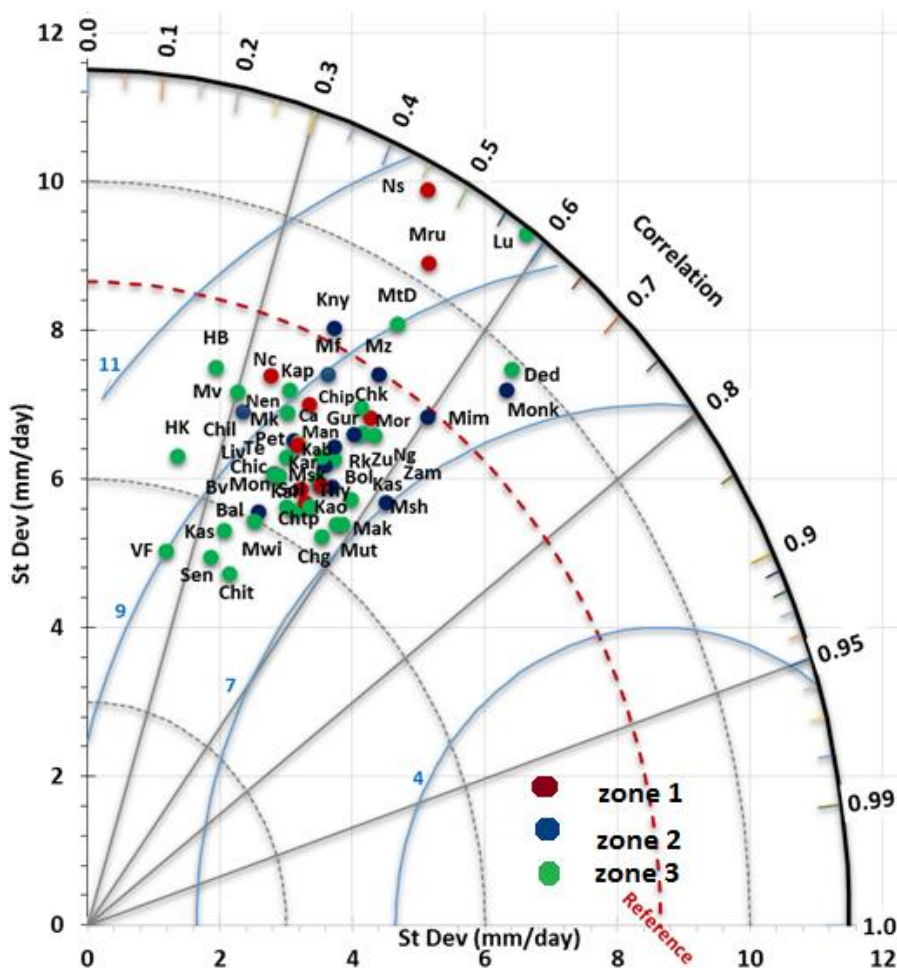
(d)

423
424
425

Figure 4: Double Mass Curves for accumulated amount of rainfall in selected suspicious raingauges. Top left panes: Nchalo vs Nsanje, Makhanga, Ngabu and Thylo. Top right: Neno vs Monkey, Balaka, Chileka, Makoka and Mimosa. Bottom left: Mvurwi vs Mt Darwin, Muzarabani, Guruve and Karoi. Bottom right: Bolero vs Chitipa, Mfuwe, Lundazi and Kasungu

426 **4.3. Elevation influences: CMORPH and gauge rainfall**

427 A Taylor Diagram with a comparison of the daily averaged time series (1998–2013) CMORPH
 428 and rain gauge observations for the 3 elevation zones is shown in Figure 5. The diagram was
 429 prepared with the **adjusted** rainfall stations (Petauke, Harare Kutsaga, Bolero, Mvurwi,
 430 Kanyemba, Neno and Nchalo) to show if the relation between CMORPH and gauge rainfall is
 431 elevation dependent. Nearly 90 % (47 out of 54) of the stations fall below the reference mean
 432 standard deviation (8.45 mm/day). **It can be noted that 16 % (5 out of 31) of the stations in the**
 433 **highland area (>1600 m) have a standard deviation below 6 mm/day indicating low variability**
 434 **in their data. In addition 25 % (2 out of 8) of the stations in the lower elevation zone (<250 m)**
 435 **are above the reference 8.4 mm/day standard deviation and, as such, indicate high variability**
 436 **in the data. Kanyemba, Muzarabani and Mimosa stations in the intermediate elevation zone**
 437 **(250-950 m) lie on the dashed arc (line of standard deviation) and implies matching standard**
 438 **deviation with gauged based estimates. However, no station is close to the indicated reference**
 439 **point implying that the whole basin has low correlation and low RMSE.**
 440



441 Figure 5. Normalised statistical comparison between time series of Rain gauge (reference) vs CMORPH estimations, period
 442 1998-2013, for the 54 rain gauge stations. Refer to Table 1 for full names of the stations. The correlation coefficients for the
 443 radial line denote the relationship between CMORPH and gauge based observations. Standard deviations on the x and y axes
 444 show the amount of variance between the two time series. The distance of the symbol to the origin depicts the ratio of
 445 CMORPH standard deviation to Rain gauge standard deviation. The angle between symbol and abscissa measures the
 446 correlation between CMORPH and Rain gauge observations. The distance of the symbol from point (1, 0) is a relative measure
 447 of the CMORPH error (for details, see Taylor (2001)).
 448

449

450 All the stations have a RMSE above 7 mm/day with higher values (> 10 mm/day) found at
451 Nsanje and Harare (Belvedere). Results are also consistent with findings in West Africa's
452 Benin and Niger where the daily mean RMSE between CMORPH and gauge based
453 measurements for a period ranging from 2003-2009, was found to be 9 mm/day and 13.8
454 mm/day, respectively (Gosset et al., 2013). Overall the CMORPH performance in terms of
455 correlation coefficient, RMSE and standard deviation over the 3 elevation zones does not
456 follow a specific pattern even though the high lying stations show a slightly better match to
457 CMORPH estimates. We can conclude that aspects of elevation in the Zambezi Basin are not
458 well shown in the relationship between CMORPH and gauge rainfall. This finding is also
459 described in Vernimmen et al. (2012) in Indonesia who found no relationship between
460 performance of TMPA 3B42RT precipitation against and elevation ($R^2 = 0.0001$). The study
461 by Gao and Liu (2013) showed that the bias in CMORPH rainfall over the Tibetan Plateau
462 present weak dependence on topography. Contrary to these findings, Romilly and
463 Gebremichael (2011) showed that the accuracy at a monthly scale of high resolution SREs:
464 CMORPH, PERSIANN and TRMM TMPA 3B42RT is related to elevation for six river basins
465 in Ethiopia. This difference could be due to the fact that the range of elevation in Ethiopia is
466 from minus 196 m to 4 500 m asl. (Romilly and Gebremichael, 2011). In contrast, the Zambezi
467 basin stations used in this study have elevation ranges from 3m to 1 575 m asl.

468

469 **4.4. Performance of CMORPH rainfall vs Gauge estimates**

470 The spatial distribution of values of bias, Rbias, RMSE and CC are presented at (sub) basin
471 level (Figure 6-8) but also for individual stations (Table 4). Figure 6 shows the bias estimate
472 of gauge and CMORPH daily rainfall for the Zambezi Basin. Large bias values are identified
473 at Lower Zambezi stations such as Mimosa (1.57 mm/day), Thyolo (1.47 mm/day), Bvumbwe
474 (1.24 mm/day) and Chichiri (0.95 mm/day). Negative bias at Middle Zambezi stations such as
475 Mfuwe (-1.7 mm/day) and Chitedze (-0.9 mm/day) indicates rainfall underestimation.
476 Generally CMORPH overestimates rainfall estimates at 9 stations (33 %) of the Lower
477 Zambezi. Most of these Lower Zambezi stations are in south eastern part of the basin in
478 Mozambique where the Zambezi Basin enters the Indian Ocean. CMORPH overestimates daily
479 rainfall estimates at 7 out of 10 stations in the Upper Zambezi stations of which most are at
480 high elevated areas. Most of these highland stations are in Zambezi's Kabompo Basin, the
481 headwater catchment of the Zambezi to the West. Overall, data for stations in the Middle
482 Zambezi Basin underestimates rainfall based on basin average bias (-0.12 mm/day).

483

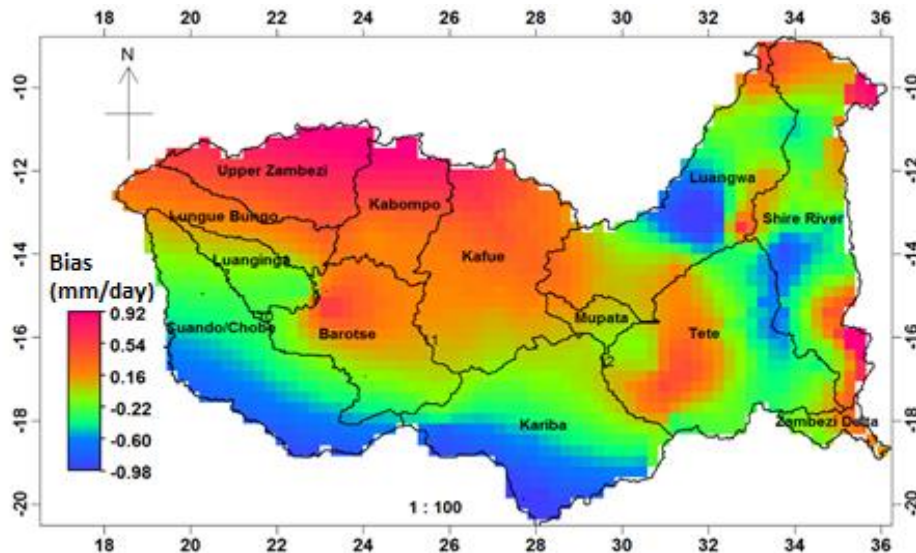


Figure 6: Bias estimate of gauge and CMORPH daily rainfall for the Zambezi Basin

484
485
486

487 Figure 7 shows that a number of stations such as Nchalo in the Lower Zambezi and Karoi in
488 the Middle Zambezi have Rbias relatively close to zero, -2.24 mm/day and, 1.17 mm/day,
489 respectively (see also Table 4). CMORPH accurately estimates rainfall at these stations.
490 Stations such as Tyolo, Mimosa and Victoria Falls have very high Rbias (>40 mm/day) and
491 indicates that the daily rainfall of this product does not correspond well with the observed
492 rainfall. It is worth noting that there is overestimation at 70 % of the stations (19 out of 27
493 stations) of the Lower Zambezi areas. There is overestimation at 35 % of the stations (6 out of
494 17 stations) in the Middle Zambezi stations. All the 10 stations in the Upper Zambezi are
495 overestimating rainfall (>7mm/day). Note that the basin mean for the Middle Zambezi stations
496 is as low as -0.59 compared to 14.32 for the Upper Zambezi and 11.24 for the Lower Zambezi.
497

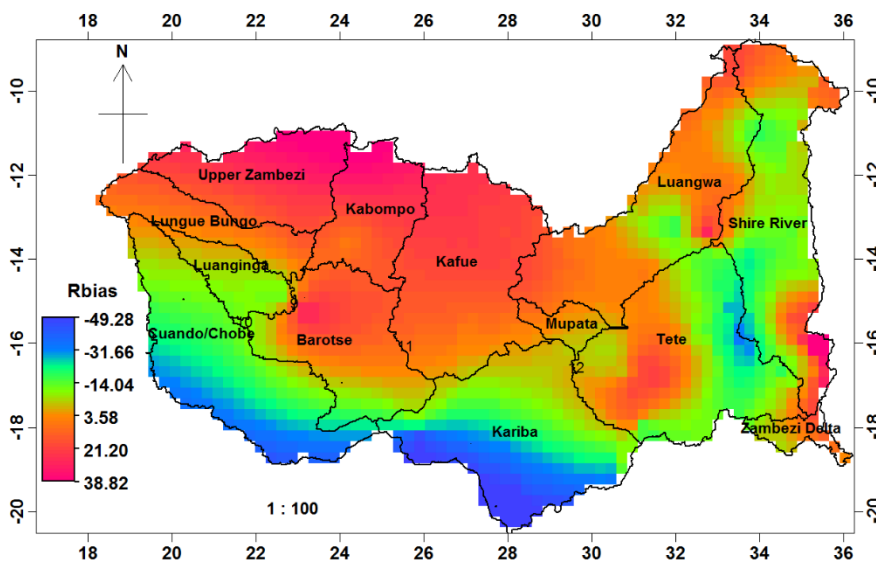
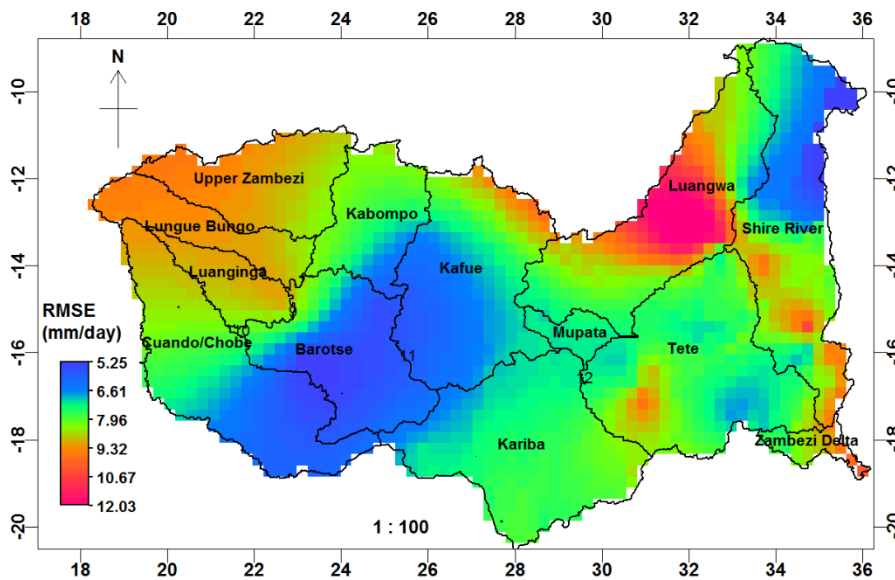


Figure 7: Rbias estimate of gauge and CMORPH daily rainfall for the Zambezi Basin

498
499
500

501 The lowest RMSE (Figure 8) is found in highland stations of the Upper Zambezi such as
502 Senanga (4.99 mm/day) and this suggest that CMORPH rainfall matches the gauge based

503 estimates. This is comparable to the lowest RMSE found in the Lower Zambezi's lowland
 504 stations such as Mfuwe (6.41 mm/day). Studies such by Moazami et al. (2013) in Iran
 505 demonstrated more accurate estimations of satellite rainfall in highland and mountainous areas
 506 than in lowland areas. Contrary to our findings, some studies report that satellite rainfall
 507 estimations have much smaller error in lowland areas than in mountainous regions
 508 (Gebregiorgis and Hossain, 2013; Stampoulis and Anagnostou, 2012).
 509



510
 511 Figure 8: RMSE estimate of gauge and CMORPH daily rainfall for the Zambezi Basin

512
 513 The generally poor performance by CMORPH shown by some of the performance indicators
 514 suggest that satellite estimates do not provide results similar to the gauge measurements. This
 515 could be a result of both the temporal and the spatial samples being different. In addition, the
 516 low spatial coverage (e.g. for Angola to the NW of Zambezi Basin) could have contributed to
 517 poor representation of the above skills over large areas.
 518

519 4.5. Rainfall bias correction

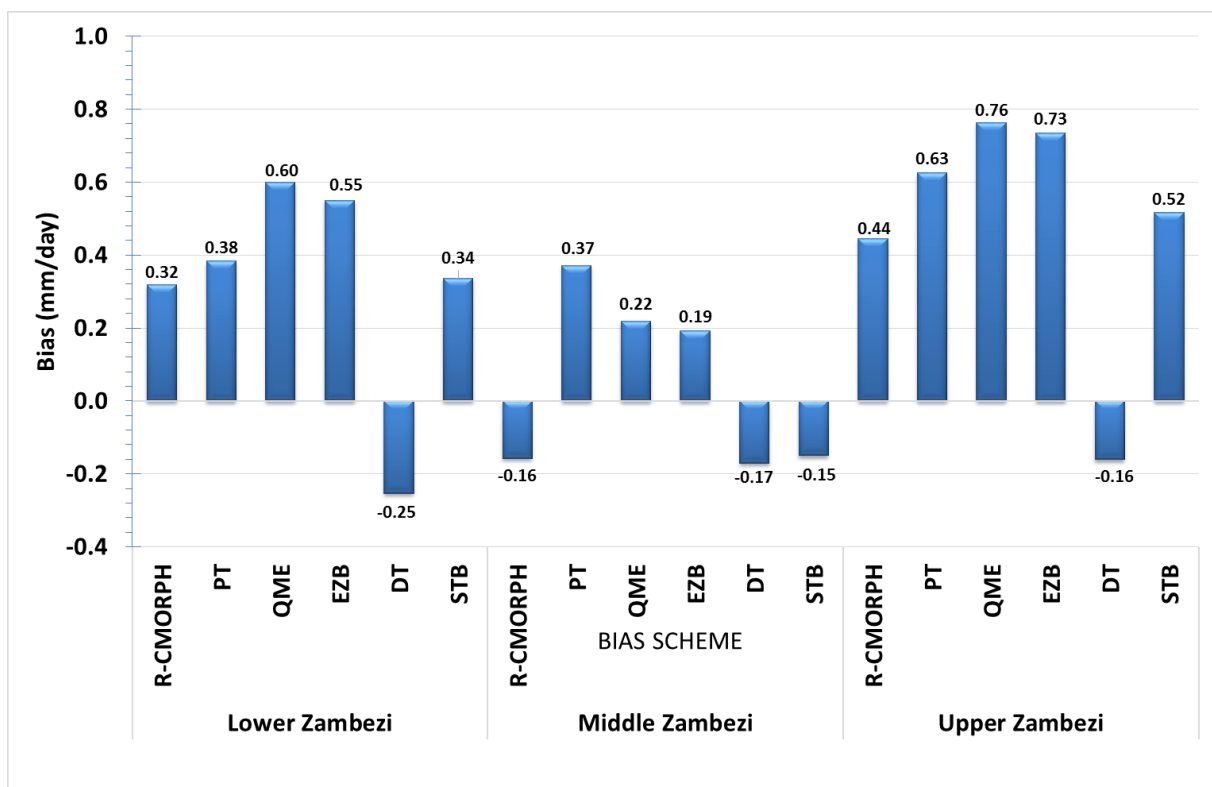
520 The statistics for the gauge, uncorrected and bias corrected satellite rainfall types for each of
 521 the Zambezi basins are shown in Table 4. The Spatio-temporal bias (STB) and Distribution
 522 transformation (DT) bias correction schemes are effective in correcting for the mean values of
 523 the CMORPH estimations. The Power transform (PT) in the Lower Zambezi, STB in the Middle
 524 Zambezi and DT in the Upper Zambezi have standard deviations closer to the gauge
 525 observations than all other bias correction schemes. The PT also has the closest maximum
 526 rainfall estimates to the gauge observations in the Lower and Middle Zambezi Basins as
 527 compared to greater overestimation by other bias correction schemes (e.g. STB: 216 mm/day
 528 vs Gauge: 107 mm/day). Our results are consistent with findings by Ahmed et al (2015) who
 529 showed that PT is the most reliable and suitable method for removing bias in GCM model
 530 derived monthly rainfall in an arid Baluchistan mountainous province of Pakistan. In the Lower

531 and Upper Zambezi basins, the DT total volume of rainfall is closer to the gauge observations
 532 and suggests effectiveness of the bias correction scheme. In the Middle Zambezi Basin, the
 533 uncorrected CMORPH (R-CMORPH) actually performs better than the bias correction schemes
 534 in reproducing the total rainfall volume. Underestimation of runoff volume is experienced for
 535 most bias correction schemes as shown by ratios of less than 1.0. Using the standard statistics,
 536 it can be observed that the DT bias correction scheme was effective in removing bias in the
 537 CMORPH rainfall particularly in the Upper Zambezi basin. However we observe that the bias
 538 schemes performance depends on the original aim they are designed for. For example the STB
 539 and PT are meant to adjust the mean and standard deviations of CMORPH rainfall estimates
 540 respectively. Statistics in Table 4 for the 3 Zambezi basins confirm these findings.

541
 542 Table 4: HERE

544 Figure 9 shows generally high bias values of the six bias correction schemes for the Upper
 545 Zambezi Basin. The highest bias range (-0.38 to 0.46 mm/day) is found in the Middle Zambezi
 546 Basin. The negative bias prevalent for the DT bias correction scheme in all the three Zambezi
 547 basins suggests underestimation of rainfall while the rest tend to generally overestimate.

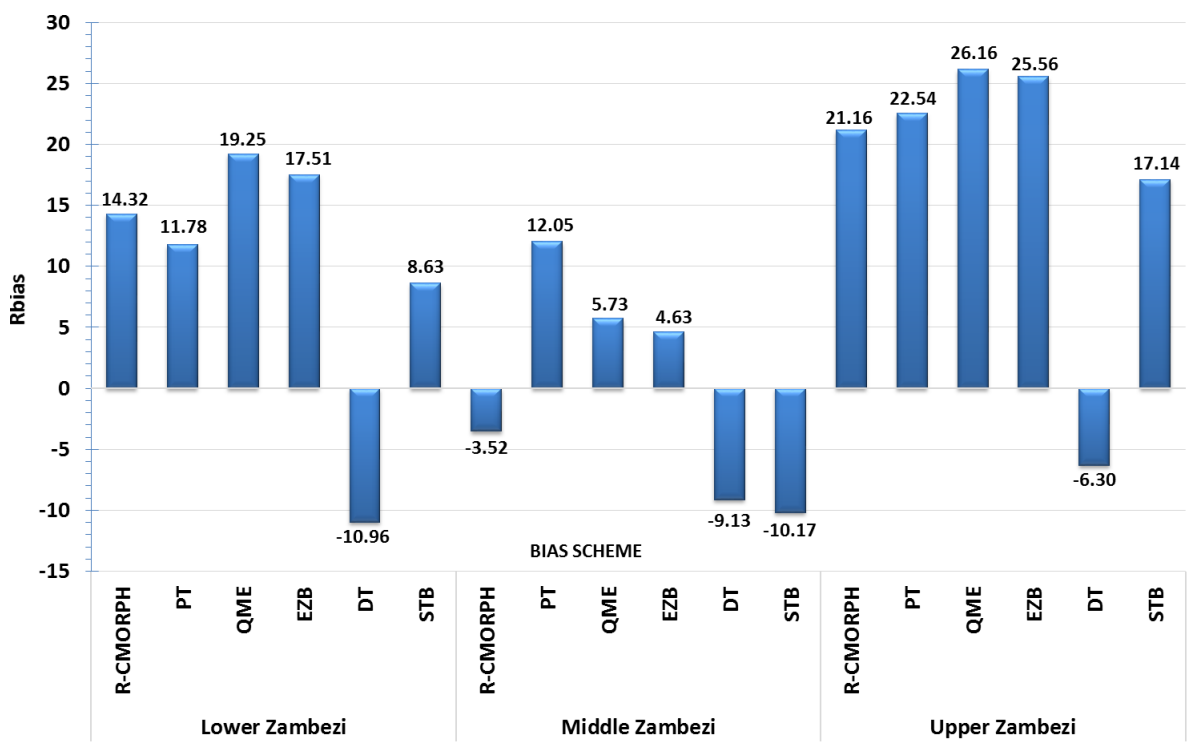
548



549
 550 Figure 9: Bias values of gauge and CMORPH daily rainfall for the uncorrected CMORPH and the 5 bias correction schemes
 551 averaged for the Lower Zambezi, Middle Zambezi and Upper Zambezi.
 552

553 The highest Rbias is consistently found for the EZB bias correction scheme. Significant
 554 underestimation of rainfall is by DT for the Lower and Middle Zambezi Basin (Figure 10). The

555 most significant skill in reproducing gauge based estimates (-17.06) is captured in the Middle
 556 Zambezi Basin for all the bias correction schemes save for DT
 557
 558



559
 560 Figure 10: Rbias of gauge and CMORPH daily rainfall for the uncorrected CMORPH and the 5 bias correction schemes
 561 averaged for the Lower Zambezi, Middle Zambezi and Upper Zambezi.
 562
 563

564 Based on the RMSE, the best performing bias correction scheme for the Lower, Middle and
 565 Upper Zambezi basin is DT, EZB and PT respectively. The lower the RMSE score, the less
 566 difference there is between the bias corrected CMORPH and gauge based estimates (Figure
 567 11). The most unsatisfactory performing bias correction scheme is PT for the lower Zambezi
 568 (10.10 mm/day). This RMSE is even poorer compared to the uncorrected CMORPH (8.63
 569 mm/day) and shows the ineffectiveness of the bias correction scheme.
 570

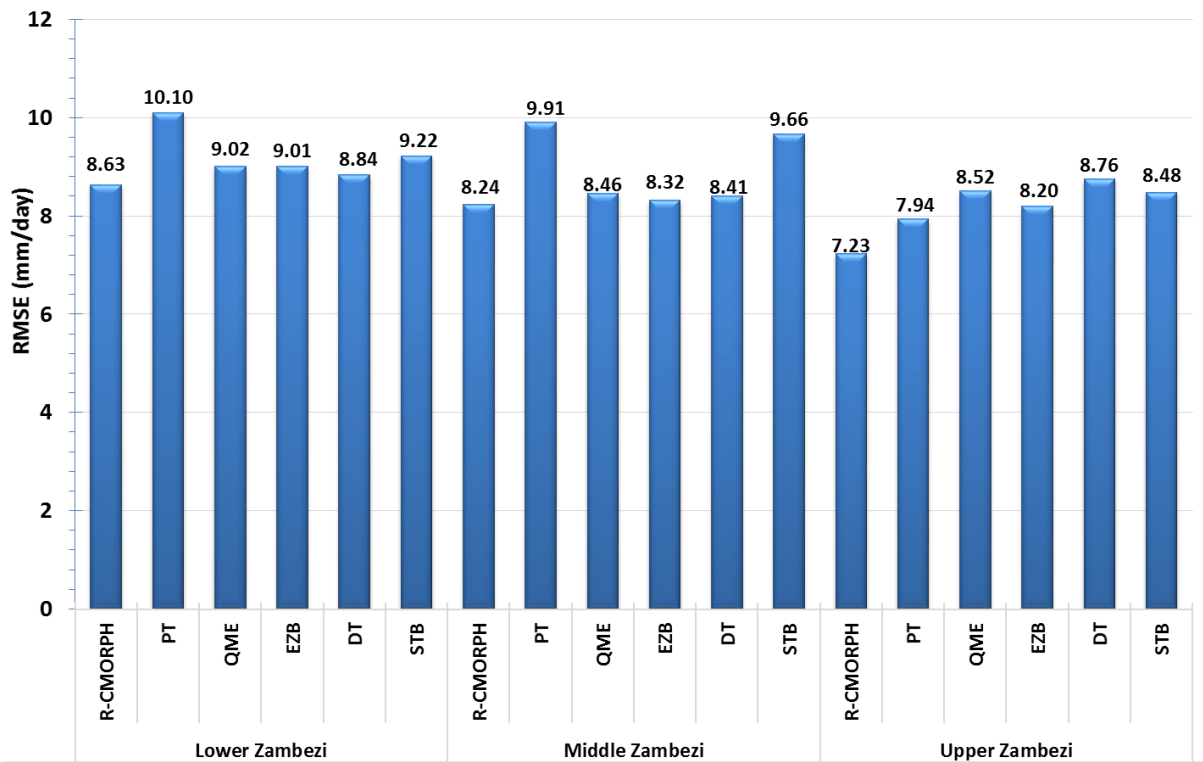
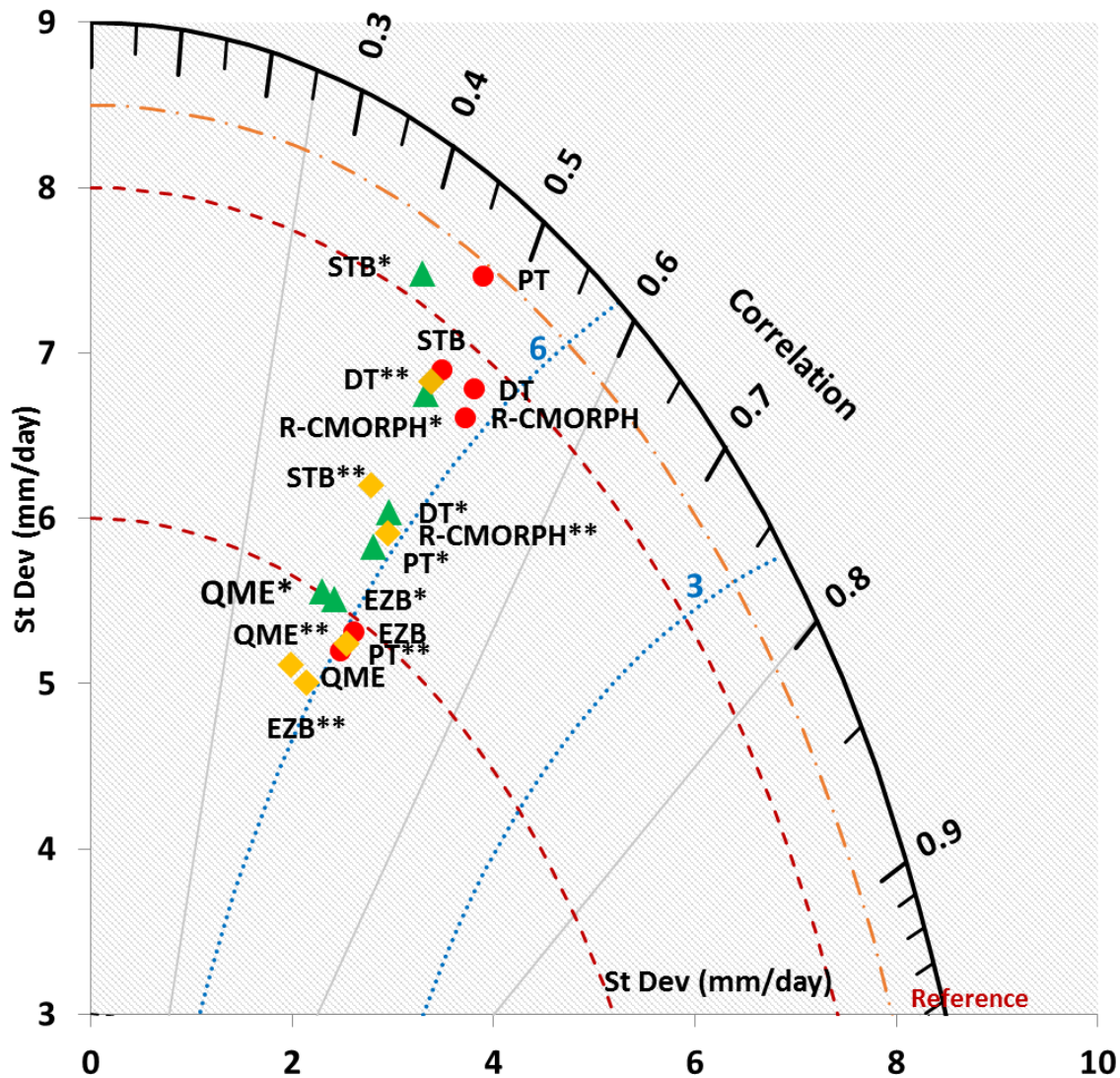


Figure 11: RMSE of CMORPH daily rainfall for the uncorrected CMORPH and the 5 bias correction schemes averaged for the Lower Zambezi, Middle Zambezi and Upper Zambezi.

571
572
573
574

575 Figure 12 shows the Taylor diagram statistical comparison between the time series of rain
576 gauge (reference) observations vs CMORPH bias correction schemes averaged for the Lower
577 Zambezi, Middle Zambezi and Upper Zambezi for the period 1998-2013. There is no data for
578 any bias correction scheme that lies closer to the reference point on the X-axis suggesting the
579 overall ineffectiveness of the bias correction schemes in removing errors. Only the PT for the
580 Lower Zambezi basin lie on the dashed arc (line of standard deviation) and means they have
581 the correct standard deviation which indicates that the pattern variations are of the right
582 amplitude. There is no consistent pattern of variability in the bias correction schemes. However
583 gauged against the reference raingauge mean standard deviation of 8.5 mm/day, most bias
584 correction schemes exhibit high variability in CMORPH performance across all the Zambezi
585 basins.

586



587
 588 Figure 12: Taylor's diagram of statistical comparison between the time series of Rain gauge (reference) observations vs
 589 CMORPH bias correction schemes averaged for the Lower Zambezi, Middle Zambezi and Upper Zambezi for the period 1998-
 590 2013. The distance of the symbol from point (1, 0) is a relative measure of the bias correction scheme's error. The position of
 591 each symbol appearing on the plot quantifies how closely that bias correction scheme's precipitation pattern matches the
 592 rain gauge. Lower Zambezi=no asterisk, Middle Zambezi=*, Upper Zambezi = **. The blue contours indicate the RMSE
 593 values.

594
 595 Most of the bias correction schemes lie in the range 6.0 to 9.0 mm/day (Figure 12). There is a
 596 consistent pattern between the bias correction schemes that have low correlation and high
 597 RMSE. Overall, the best performing bias correction schemes (DT and PT) have CC close to
 598 0.5, standard deviation close to the reference (8.5 mm/day) and a RMSE less than 6mm/day.
 599 This is mainly for the Lower and Middle Zambezi basins showing a fair agreement with gauge
 600 based estimates and also an effectiveness of this bias correction scheme. The least performing
 601 bias correction scheme is QME and EZB with a low CC < 0.43 and standard deviation (< 6.0)
 602 that is lower than the reference suggesting poor skill of these bias correction schemes. Inherent
 603 to the methodology of most of the bias correction schemes (e.g. DT and QME) is that the spatial
 604 pattern of the SRE does not change and therefore the correlation for a specific station for daily
 605 precipitation does not necessarily improve.

606

607 The percentage of days belonging to the five rainfall intensities in the Zambezi basin for each
608 bias correction scheme is shown in Table 5. The greater percentage of rainfall (>82 %) falls
609 under the very light shower rains, 0-2.5 mm/day. A smaller percentage falls under the 2.5-5.0
610 mm/day which are the fairly light showers. A very low percentage belongs to the heavy showers
611 of greater than 20 mm/day. Compared to the gauge based estimates, the STB, PT and DT
612 generally resembles the gauge based estimates in terms of the five rainfall intensities in all the
613 Zambezi basins and this presents the effectiveness of the three bias correction schemes. All the
614 five rainfall types in the Lower and Middle Zambezi basins generally tend to overestimate the
615 moderately heavy rainfall (10–20 mm/day) and underestimate moderate and heavy rainfall (>20
616 mm). Results are consistent with findings by Gao and Liu (2013) who also found consistent
617 under and overestimation in the Tibetan Plateau by monthly high-resolution precipitation
618 products including CMORPH for almost the same rainfall range (>10mm/day).

619

620 Table 5: HERE

621

622

623 **4.6. Seasonality influences on CMORPH bias correction**

624 Table 6 shows standard statistics for the gauge, uncorrected and bias corrected satellite rainfall
625 for the dry and wet seasons. Compared to the gauge based and uncorrected CMORPH, the
626 Distribution transformation (DT) and Spatio-temporal bias (STB) schemes are more effective
627 in correcting errors in satellite rainfall than the Power transform (PT), Elevation Space bias
628 (EZB) and Quantile based empirical-statistical error correction method (QME). The DT is more
629 effective in reducing bias in the dry season than the wet season. For both the wet and dry
630 season, the STB is most effective in reducing bias in the Upper Zambezi Basin. This result
631 agrees with findings in Ines and Hansen (2006) for semi-arid eastern Kenya which showed that
632 multiplicative bias correction schemes (in this case STB) were effective in correcting monthly
633 and seasonal rainfall totals.

634

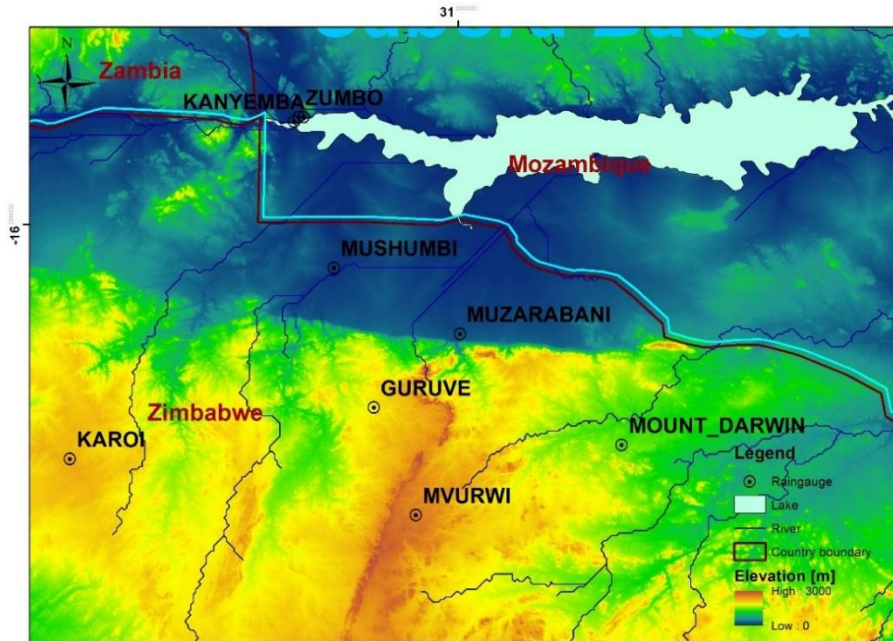
635

636 Table 6: HERE

637

638 **4.7. Elevation influences on CMORPH bias correction**

639 Using the elevation space (EZB) bias correction scheme, bias correction effectiveness at the
640 Zambezi escarpment (highland) and valley (lowland) of the Middle Zambezi Basin (Figure 13)
641 was assessed. We took a closer look at 6 stations, of which 3 (Mushumbi, Zumbo and
642 Kanyemba) are on the Zambezi escarpment with elevation above 1 100 m and the other 3
643 (Mvurwi, Guruve, Karoi) in the valley have an elevation below 400 m. The stations have an
644 mean distance between gauges of about 105 km.



645
646 **Figure 13: Location of stations and elevation of the Zambezi valley and escarpment**

647
648 Table 7 reveals that for the uncorrected CMORPH, the rainfall data for stations in the valley
649 has serious underestimation of rainfall than for the escarpment, save for Guruve station.
650 Through EZB bias correction scheme, rainfall data for the stations on the Zambezi escarpment
651 have effectively reduced the bias and Rbias in CMORPH rainfall than for stations on the
652 escarpment. None of the valley stations' rainfall nor their escarpment counterparts were
653 effective in reducing the RMSE. However, the CC slightly reduced for all the six stations after
654 bias correction. The general conclusion is that rainfall data for stations in the Zambezi valley
655 outperform that of stations on the escarpment in terms of uncorrected CMORPH performance
656 and its bias correction.

657
658 Table 7. HERE

659
660
661 **5. Conclusions**

662
663 Rainfall in semi-arid river basins such as the Zambezi plays a central role in the livelihoods of
664 human populations. The adoption of SREs offers a timely and cost efficiency opportunity to
665 improve our understanding of the spatio-temporal variation of this water cycle component. The
666 above is important for instance for climate monitoring, hydrologic prediction, model
667 verification, or any other application that affect land or water management where rainfall data
668 is required. Since SREs are prone to systematic and random errors by the fact that SREs are
669 indirect rainfall estimates, this study aimed to to assess suitability of bias correction of
670 CMORPH satellite rainfall estimates in the Zambezi River Basin for the period 1998-2013 for
671 which time series are available from 54 rain gauge stations. From the study, the following can
672 be concluded:

- 674 1. Quality control performed on the gauge based estimates in the Zambezi Basin helped to
675 improve reliability of gauge based estimates. Uncorrected CMORPH rainfall estimates in
676 the three Zambezi subbasins show inconsistencies (in terms of rainfall volume, depth and
677 intensity) when compared with gauge based estimates. Results also show that it is not
678 always the case that the Lower, Middle or Upper Zambezi station estimations outperform
679 one another. Analyses showed that the aspects of elevation in the Zambezi Basin are not
680 well shown in the relationship between CMORPH and gauge rainfall. Findings from this
681 study agree with previous work by Gao and Liu (2013) and Vernimmen et al. (2012) who
682 found weak relationship between performance of SREs and elevation. The research yet
683 contradict previous observations (e.g. Haile et al., 2009;Katiraie-Boroujerdy et al.,
684 2013;Rientjes et al., 2013;Wu and Zhai, 2012) that found elevation dependant trends of
685 CMORPH rainfall distribution. This shows that there is still room for further research in
686 this area.
687
- 688 2. The additive bias correction scheme (Distribution transformation) has the best estimation
689 of rainfall particularly in the Upper Zambezi Basin. However each bias correction factor
690 has its desirable outcome depending on the performance indicators used. The linear based
691 (Spatio-temporal) bias correction scheme successfully adjusted the daily mean of
692 CMORPH estimates at 70 % of the stations and was also more effective in reducing the
693 rainfall bias. The spatio-temporal bias correction scheme, using gauge and or SREs bias
694 values that vary over time over the entire Zambezi basin is more effective in reducing
695 rainfall bias than the EZB that does not consider spatial variation. The nonlinear bias
696 correction schemes (Power transform and the Quantile based empirical-statistical error
697 correction method) were more effective in reproducing the rainfall totals.
698
- 699 3. The study assessed the percentage of days belonging to the five rainfall intensities (0-2.5,
700 2.5-5, 5-10, 10-20 and >20 mm/day) in the Zambezi basin for each bias correction scheme.
701 There is overestimation of the moderately heavy rainfall (10–20 mm/day) and
702 underestimation of the moderate to heavy rainfall (>20 mm) by the five bias corrected
703 rainfall types. Overall improved performance was experienced through the STB, PT and
704 DT schemes.
705
- 706 4. Detailed analysis for stations in the Zambezi valley (< 400 m amsl) and escarpment (> 1
707 100 m amsl) indicate that bias correction of CMORPH rainfall is influenced by elevation.
708 In addition, there is also seasonality tendencies are evident in the performance of bias
709 correction schemes. The DT is more effective in reducing bias in the dry season than the
710 wet season.
711

712 **Acknowledgements**

713 The study was supported by WaterNet through the DANIDA Transboundary PhD Research in
714 the Zambezi Basin and the University of Twente's ITC Faculty. The authors acknowledge the
715 University of Zimbabwe's Civil Engineering Department for the platform to carry out this
716 research.

717

718 **Author Contributions**

719 W.G. was responsible for the development of bias correction schemes in the Zambezi basin.
720 T.R. was responsible for the research approach and conceptualization and quality control on
721 the raingauges. A.T.H. was responsible for synthesising the methodology and made large
722 contributions to the manuscript write-up. H.M. provided some of the raingauge data and related
723 findings of this study to previous work in the Zambezi Basin. P.R. assisted in interpretation of
724 bias correction results.

725

726 **Conflict of Interests**

727

728 The authors declare no conflict of interests.

729

730 **References**

- 731 Ahmed, K., Shahid, S., Harun, S., and Nawaz, N.: Performance Assessment of Different Bias
732 Correction Methods in Statistical Downscaling of Precipitation, *Malaysian Journal of*
733 *Civil Engineering* 27 311-324, 2015.
- 734 Anagnostou, E. N., Krajewski, W. F., and Smith, J.: Uncertainty quantification of mean-areal
735 radar-rainfall estimates, *Journal of Atmospheric and Oceanic Technology*, 16, 206,
736 1999.
- 737 Bajracharya, S. R., Shrestha, M. S., and Shrestha, A. B.: Assessment of high-resolution satellite
738 rainfall estimation products in a streamflow model for flood prediction in the Bagmati
739 basin, Nepal, *Journal of Flood Risk Management*, n/a-n/a, 10.1111/jfr3.12133, 2014.
- 740 Beilfuss, R., Dutton, P., and Moore, D.: Landcover and Landuse change in the Zambezi Delta,
741 in: *Zambezi Basin Wetlands Volume III Landuse Change and Human impacts*, Chapter
742 2, Biodiversity Foundation for Africa, Harare, 31-105, 2000.
- 743 Beilfuss, R.: *A Risky Climate for Southern African Hydro: Assessing hydrological risks and*
744 *consequences for Zambezi River Basin dams*, 2012.
- 745 Beyer, M., Wallner, M., Bahlmann, L., Thiemig, V., Dietrich, J., and Billib, M.: Rainfall
746 characteristics and their implications for rain-fed agriculture: a case study in the Upper
747 Zambezi River Basin, *Hydrological Sciences Journal*, null-null,
748 10.1080/02626667.2014.983519, 2014.
- 749 Bitew, M. M., and Gebremichael, M.: Evaluation of satellite rainfall products through
750 hydrologic simulation in a fully distributed hydrologic model, *Water Resources*
751 *Research*, 47, 2011.
- 752 Bitew, M. M., Gebremichael, M., Ghebremichael, L. T., and Bayissa, Y. A.: Evaluation of
753 High-Resolution Satellite Rainfall Products through Streamflow Simulation in a
754 Hydrological Modeling of a Small Mountainous Watershed in Ethiopia, *Journal of*
755 *Hydrometeorology*, 13, 338-350, 10.1175/2011jhm1292.1, 2011.
- 756 Botter, G., Porporato, A., Rodriguez-Iturbe, I., and Rinaldo, A.: Basin-scale soil moisture
757 dynamics and the probabilistic characterization of carrier hydrologic flows: Slow,

758 leaching-prone components of the hydrologic response, *Water Resources Research*, 43,
759 n/a-n/a, 10.1029/2006WR005043, 2007.

760 Bouwer, L. M., Aerts, J. C. J. H., Van de Coterlet, G. M., Van de Giessen, N., Gieske, A., and
761 Manaerts, C.: Evaluating downscaling methods for preparing Global Circulation Model
762 (GCM) data for hydrological impact modelling. Chapter 2, in Aerts, J.C.J.H. &
763 Droogers, P.
764 (Eds.), *Climate Change in Contrasting River Basins: Adaptation Strategies for Water, Food
765 and Environment*. (pp. 25-47). Wallingford, UK: Cabi Press., 2004.

766 Breidenbach, J. P., and Bradberry, J. S.: Multisensor Precipitation Estimates Produced by
767 National Weather Service River Forecast Centers for Hydrologic Applications,
768 Proceedings of the 2001 Georgia Water Resources Conference, April 26 and 27, 2001,
769 Athens, Georgia, 2001,

770 Cheema, M. J. M., and Bastiaanssen, W. G. M.: Local calibration of remotely sensed rainfall
771 from the TRMM satellite for different periods and spatial scales in the Indus Basin,
772 *Agricultural Water Management*, 97, 1541, 2010.

773 Cohen Liechti, T., Matos, J. P., Boillat, J. L., and Schleiss, A. J.: Comparison and evaluation
774 of satellite derived precipitation products for hydrological modeling of the Zambezi
775 River Basin, *Hydrol. Earth Syst. Sci.*, 16, 489-500, 2012.

776 Dinku, T., Chidzambwa, S., Ceccato, P., Connor, S. J., and Ropelewski, C. F.: Validation of
777 high-resolution satellite rainfall products over complex terrain, *International Journal of
778 Remote Sensing*, 29, 4097-4110, 10.1080/01431160701772526, 2008.

779 Fang, G. H., Yang, J., Chen, Y. N., and Zammit, C.: Comparing bias correction methods in
780 downscaling meteorological variables for a hydrologic impact study in an arid area in
781 China, *Hydrol. Earth Syst. Sci.*, 19, 2547-2559, 10.5194/hess-19-2547-2015, 2015.

782 Fylstra, D., Lasdon, L., Watson, J., and Waren, A.: Design and Use of the Microsoft Excel
783 Solver, *Interfaces*, 28, 29-55, doi:10.1287/inte.28.5.29, 1998.

784 Gao, Y. C., and Liu, M. F.: Evaluation of high-resolution satellite precipitation products using
785 rain gauge observations over the Tibetan Plateau, *Hydrol. Earth Syst. Sci.*, 17, 837-849,
786 10.5194/hess-17-837-2013, 2013.

787 Gebregiorgis, A. S., Tian, Y., Peters-Lidard, C. D., and Hossain, F.: Tracing hydrologic model
788 simulation error as a function of satellite rainfall estimation bias components and land
789 use and land cover conditions, *Water Resources Research*, 48, n/a-n/a,
790 10.1029/2011wr011643, 2012.

791 Gebregiorgis, A. S., and Hossain, F.: Understanding the Dependence of Satellite Rainfall
792 Uncertainty on Topography and Climate for Hydrologic Model Simulation, *Geoscience
793 and Remote Sensing, IEEE Transactions on*, 51, 704-718, 10.1109/tgrs.2012.2196282,
794 2013.

795 Gosset, M., Viarre, J., Quantin, G., and Alcoba, M.: Evaluation of several rainfall products
796 used for hydrological applications over West Africa using two high-resolution gauge
797 networks, *Quarterly Journal of the Royal Meteorological Society*, 139, 923-940,
798 10.1002/qj.2130, 2013.

799 Gudmundsson, L., Bremnes, J. B., Haugen, J. E., and Engen Skaugen, T.: Technical Note:
800 Downscaling RCM precipitation to the station scale using quantile mapping – a
801 comparison of methods, *Hydrol. Earth Syst. Sci. Discuss.*, 9, 6185-6201,
802 10.5194/hessd-9-6185-2012, 2012.

803 Gutjahr, O., and Heinemann, G.: Comparing precipitation bias correction methods for high-
804 resolution regional climate simulations using COSMO-CLM, *Theor Appl Climatol*,
805 114, 511-529, 10.1007/s00704-013-0834-z, 2013.

- 806 Habib, E., ElSaadani, M., and Haile, A. T.: Climatology-Focused Evaluation of CMORPH and
807 TMPA Satellite Rainfall Products over the Nile Basin, *Journal of Applied Meteorology*
808 and *Climatology*, 51, 2105-2121, 10.1175/jamc-d-11-0252.1, 2012.
- 809 Habib, E., Haile, A., Sazib, N., Zhang, Y., and Rientjes, T.: Effect of Bias Correction of
810 Satellite-Rainfall Estimates on Runoff Simulations at the Source of the Upper Blue
811 Nile, *Remote Sensing*, 6, 6688-6708, 2014.
- 812 Haile, A. T., Rientjes, T., Gieske, A., and Gebremichael, M.: Rainfall Variability over
813 Mountainous and Adjacent Lake Areas: The Case of Lake Tana Basin at the Source of
814 the Blue Nile River, *Journal of Applied Meteorology and Climatology*, 48, 1696-1717,
815 10.1175/2009JAMC2092.1, 2009.
- 816 Haile, A. T., Habib, E., and Rientjes, T. H. M.: Evaluation of the climate prediction center CPC
817 morphing technique CMORPH rainfall product on hourly time scales over the source
818 of the Blue Nile river, *Hydrological processes*, 27, 1829-1839, 2013.
- 819 Hempel, S., Frieler, K., Warszawski, L., Schewe, J., and Piontek, F.: A trend-preserving bias
820 correction – the ISI-MIP approach, *Earth Syst. Dynam.*, 4, 219-236,
821 10.5194/esd-4-219-2013, 2013.
- 822 Ines, A. V. M., and Hansen, J. W.: Bias correction of daily GCM rainfall for crop simulation
823 studies, *Agricultural and Forest Meteorology*, 138, 44-53,
824 <http://dx.doi.org/10.1016/j.agrformet.2006.03.009>, 2006.
- 825 Jiang, S., Ren, L., Hong, Y., Yong, B., Yang, X., Yuan, F., and Ma, M.: Comprehensive
826 evaluation of multi-satellite precipitation products with a dense rain gauge network and
827 optimally merging their simulated hydrological flows using the Bayesian model
828 averaging method, *Journal of Hydrology*, 452-453, 213-225,
829 <http://dx.doi.org/10.1016/j.jhydrol.2012.05.055>, 2012.
- 830 Joyce, R. J., Janowiak, J. E., Arkin, P. A., and Xie, P.: CMORPH: A method that produces
831 global precipitation estimates from passive microwave and infrared data at high spatial
832 and temporal resolution, *J. Hydromet.*, 5, 487-503, 2004.
- 833 Katirai-e-Boroujerdy, P., Nasrollahi, N., Hsu, K., and Sorooshian, S.: Evaluation of satellite-
834 based precipitation estimation over Iran, Elsevier, Kidlington, ROYAUME-UNI, 15
835 pp., 2013.
- 836 Lafon, T., Dadson, S., Buys, G., and Prudhomme, C.: Bias correction of daily precipitation
837 simulated by a regional climate model: a comparison of methods, *Int. J. Climatol.*, 33,
838 1367-1381, 10.1002/joc.3518, 2013.
- 839 Lenderink, G., Buishand, A., and van Deursen, W.: Estimates of future discharges of the river
840 Rhine using two scenario methodologies: direct versus delta approach, *Hydrol. Earth*
841 *Syst. Sci.*, 11, 1145-1159, 10.5194/hess-11-1145-2007, 2007.
- 842 Mashingia, F., Mtaló, F., and Bruen, M.: Validation of remotely sensed rainfall over major
843 climatic regions in Northeast Tanzania, *Physics and Chemistry of the Earth, Parts*
844 *A/B/C*, 67-69, 55-63, <http://dx.doi.org/10.1016/j.pce.2013.09.013>, 2014.
- 845 Matos, J. P., Cohen Liechti, T., Juárez, D., Portela, M. M., and Schleiss, A. J.: Can satellite
846 based pattern-oriented memory improve the interpolation of sparse historical rainfall
847 records?, *Journal of Hydrology*, 492, 102-116,
848 <http://dx.doi.org/10.1016/j.jhydrol.2013.04.014>, 2013.
- 849 Moazami, S., Golian, S., Kavianpour, M. R., and Hong, Y.: Comparison of PERSIANN and
850 V7 TRMM Multi-satellite Precipitation Analysis (TMPA) products with rain gauge
851 data over Iran, *International Journal of Remote Sensing*, 34, 8156-8171,
852 10.1080/01431161.2013.833360, 2013.
- 853 Müller, M. F., and Thompson, S. E.: Bias adjustment of satellite rainfall data through stochastic
854 modeling: Methods development and application to Nepal, *Advances in Water*
855 *Resources*, 60, 121-134, <http://dx.doi.org/10.1016/j.advwatres.2013.08.004>, 2013.

856 Pereira Filho, A. J., Carbone, R. E., Janowiak, J. E., Arkin, P., Joyce, R., Hallak, R., and Ramos,
857 C. G. M.: Satellite Rainfall Estimates Over South America – Possible Applicability to
858 the Water Management of Large Watersheds1, *JAWRA Journal of the American Water*
859 *Resources Association*, 46, 344-360, 10.1111/j.1752-1688.2009.00406.x, 2010.

860 Qin, Y., Chen, Z., Shen, Y., Zhang, S., and Shi, R.: Evaluation of Satellite Rainfall Estimates
861 over the Chinese Mainland, *Remote Sensing*, 6, 11649-11672, 2014.

862 Rientjes, T., Haile, A. T., and Fenta, A. A.: Diurnal rainfall variability over the Upper Blue
863 Nile Basin: A remote sensing based approach, *International Journal of Applied Earth*
864 *Observation and Geoinformation*, 21, 311-325,
865 <http://dx.doi.org/10.1016/j.jag.2012.07.009>, 2013.

866 Romilly, T. G., and Gebremichael, M.: Evaluation of satellite rainfall estimates over Ethiopian
867 river basins, *Hydrol. Earth Syst. Sci.*, 15, 1505-1514, 10.5194/hess-15-1505-2011,
868 2011.

869 Searcy, J. K., and Hardison, C. H.: Double-mass curves. U.S. Geological Survey Water-Supply
870 Paper 1541-B, 1960.

871 Seo, D. J., Breidenbach, J. P., and Johnson, E. R.: Real-time estimation of mean field bias in
872 radar rainfall data, *Journal of Hydrology*, 223, 131-147,
873 [http://dx.doi.org/10.1016/S0022-1694\(99\)00106-7](http://dx.doi.org/10.1016/S0022-1694(99)00106-7), 1999.

874 Shrestha, M. S.: Bias-adjustment of satellite-based rainfall estimates over the central
875 Himalayas of Nepal for flood prediction. PhD thesis, Kyoto University, 2011.

876 Stampoulis, D., and Anagnostou, E. N.: Evaluation of Global Satellite Rainfall Products over
877 Continental Europe, *Journal of Hydrometeorology*, 13, 588-603, 10.1175/jhm-d-11-
878 086.1, 2012.

879 Taylor, K. E.: Summarizing multiple aspects of model performance in a single diagram, *Journal*
880 *of Geophysical Research: Atmospheres*, 106, 7183-7192, 10.1029/2000JD900719,
881 2001.

882 Tesfagiorgis, K., Mahani, S. E., Krakauer, N. Y., and Khanbilvardi, R.: Bias correction of
883 satellite rainfall estimates using a radar-gauge product – a case study in
884 Oklahoma (USA), *Hydrol. Earth Syst. Sci.*, 15, 2631-2647, 10.5194/hess-15-2631-
885 2011, 2011.

886 Teutschbein, C., and Seibert, J.: Is bias correction of regional climate model (RCM)
887 simulations possible for non-stationary conditions?, *Hydrol. Earth Syst. Sci.*, 17, 5061-
888 5077, 10.5194/hess-17-5061-2013, 2013.

889 Themeßl, M. J., Gobiet, A., and Leuprecht, A.: Empirical-statistical downscaling and error
890 correction of daily precipitation from regional climate models, *Int. J. Climatol.*, 31,
891 1530-1544, 10.1002/joc.2168, 2010.

892 Themeßl, M. J., Gobiet, A., and Heinrich, G.: Empirical-statistical downscaling and error
893 correction of regional climate models and its impact on the climate change signal, *Clim.*
894 *Change*, 112, 449–468 2012.

895 Thiemiig, V., Rojas, R., Zambrano-Bigiarini, M., Levizzani, V., and De Roo, A.: Validation of
896 Satellite-Based Precipitation Products over Sparsely Gauged African River Basins,
897 *Journal of Hydrometeorology*, 13, 1760-1783, 10.1175/jhm-d-12-032.1, 2012.

898 Thiemiig, V., Rojas, R., Zambrano-Bigiarini, M., and De Roo, A.: Hydrological evaluation of
899 satellite-based rainfall estimates over the Volta and Baro-Akobo Basin, *Journal of*
900 *Hydrology*, 499, 324-338, 10.1016/j.jhydro.2013.07.012, 2013.

901 Thorne, V., Coakeley, P., Grimes, D., and Dugdale, G.: Comparison of TAMSAT and CPC
902 rainfall estimates with raingauges, for southern Africa, *International Journal of Remote*
903 *Sensing*, 22, 1951-1974, 10.1080/01431160118816, 2001.

904 Tian, Y., Peters-Lidard, C. D., and Eylander, J. B.: Real-Time Bias Reduction for Satellite-
905 Based Precipitation Estimates, *Journal of Hydrometeorology*, 11, 1275-1285,
906 10.1175/2010JHM1246.1, 2010.

907 Toté, C., Patricio, D., Boogaard, H., van der Wijngaart, R., Tarnavsky, E., and Funk, C.:
908 Evaluation of Satellite Rainfall Estimates for Drought and Flood Monitoring in
909 Mozambique, *Remote Sensing*, 7, 1758, 2015.

910 Tumbare, M. J.: Management of River Basins and Dams: The Zambezi River Basin, edited by:
911 Tumbare, M. J., Taylor & Francis, 318 pp., 2000.

912 Tumbare, M. J.: The Management of the Zambezi River Basin and Kariba Dam, Bookworld
913 Publishers, Lusaka, 2005.

914 Vernimmen, R. R. E., Hooijer, A., Mamenun, Aldrian, E., and van Dijk, A. I. J. M.: Evaluation
915 and bias correction of satellite rainfall data for drought monitoring in Indonesia, *Hydrol.*
916 *Earth Syst. Sci.*, 16, 133-146, 10.5194/hess-16-133-2012, 2012.

917 Woody, J., Lund, R., and Gebremichael, M.: Tuning Extreme NEXRAD and CMORPH
918 Precipitation Estimates, *Journal of Hydrometeorology*, 15, 1070-1077, 10.1175/jhm-d-
919 13-0146.1, 2014.

920 World Bank: The Zambezi River Basin: A Multi-Sector Investment Opportunities Analysis,
921 Volume 2 Basin Development Scenarios, 2010a.

922 World Bank: The Zambezi River Basin : A Multi-Sector Investment Opportunities Analysis -
923 Summary Report. World Bank. © World Bank.
924 <https://openknowledge.worldbank.org/handle/10986/2958> License: Creative
925 Commons Attribution CC BY 3.0., 2010b.

926 Wu, L., and Zhai, P.: Validation of daily precipitation from two high-resolution satellite
927 precipitation datasets over the Tibetan Plateau and the regions to its east, *Acta Meteorol*
928 *Sin*, 26, 735-745, 10.1007/s13351-012-0605-2, 2012.

929 Yin, Z. Y., Zhang, X., Liu, X., Colella, M., and Chen, X.: An assessment of the biases of
930 satellite rainfall estimates over the tibetan plateau and correction methods based on
931 topographic analysis, *Journal of Hydrometeorology*, 9, 301, 2008.

932
933

934 LIST OF TABLES

935

936 Table 1: Rain gauge stations in the Zambezi Basin showing station code, subbasin they belong to, years of data availability
937 and elevation.

Station	Code	Subbasin	Zambezi classification	X Coord	Y Coord	Start date	End Date	% gaps (missing records)	Elevation (m)
Marromeu	Mru	Zambezi	Lower Zambezi	36.95	-18.28	29/05/2007	31/12/2013	0.37	3
	Ca	Delta	Lower Zambezi						
Caia		Delta		35.38	-17.82	29/05/2007		0.13	28
Nsanje	Ns	Shire	Lower Zambezi	35.27	-16.95	01/01/1998	31/12/2013	3.49	39
Makhanga	Mk	Shire	Lower Zambezi	35.15	-16.52	01/01/1998	31/12/2013	9.43	48
Nchalo	Nc	Shire	Lower Zambezi	34.93	-16.23	01/01/1998	31/12/2013	0.60	64
Ngabu	Ng	Shire	Lower Zambezi	34.95	-16.50	01/01/1998	31/12/2010	0.74	89
Chikwawa	Chk	Shire	Lower Zambezi	34.78	-16.03	01/01/1998	31/12/2010	0.93	107
Tete	Te	Tete	Lower Zambezi	33.58	-16.18	29/05/2007	31/12/2013	0.17	151
Chingodzi	Chg	Shire	Lower Zambezi	34.63	-16.00	29/05/2007	10/01/2013	11.8	280
Zumbo	Zu	Shire	Lower Zambezi	30.45	-15.62	29/05/2007	12/09/2012	0.16	345
Mushumbi	Msh	Kariba	Middle Zambezi	30.56	-16.15	11/06/2008	11/12/2013	7.47	369
Kanyemba	Kny	Tete	Middle Zambezi	30.42	-15.63	01/01/1998	30/03/2013	5.86	372
	Mor	Zambezi	Lower Zambezi						
Morrumbala		Delta		35.58	-17.35	29/05/2007	10/01/2013	13.3	378
Muzarabani	Mz	Tete	Middle Zambezi	31.01	-16.39	01/01/1998	31/12/2013	1.14	430

Monkey	Mon	Shire	Lower Zambezi	34.92	-14.08	01/01/1998	30/11/2010	0.00	478
Mangochi	Man	Shire	Lower Zambezi	35.25	-14.47	01/01/1998	31/12/2010	0.02	481
Rukomechi	Rk	Kariba	Middle Zambezi	29.38	-16.13	01/01/1998	31/12/2013	6.40	530
Mutarara	Mut	Shire	Lower Zambezi	33.00	-17.38	29/05/2007	10/01/2013	11.7	548
Mfuwe	Mf	Luangwa	Middle Zambezi	31.93	-13.27	01/01/1998	31/12/2010	2.70	567
Mimosa	Mim	Shire	Lower Zambezi	35.62	-16.07	01/01/1998	31/12/2010	3.96	616
Balaka	Bal	Shire	Lower Zambezi	34.97	-14.98	01/01/1998	30/04/2010	0.78	618
Thyolo	Thy	Shire	Lower Zambezi	35.13	-16.13	01/01/1998	31/12/2010	0.11	624
Chileka	Chil	Shire	Lower Zambezi	34.97	-15.67	01/01/1998	31/12/2013	0.60	744
Neno	Nen	Shire	Lower Zambezi	34.65	-15.40	01/01/1998	01/01/2010	9.14	903
Mt Darwin	MtD	Tete	Middle Zambezi	31.58	-16.78	01/01/1998	02/03/2008	5.00	962
Chipata	Chip	Shire	Lower Zambezi	32.58	-13.55	01/01/1998	13/08/2003	1.11	995
Makoka	Mak	Shire	Lower Zambezi	35.18	-15.53	01/01/1998	31/12/2010	0.00	996
Livingstone	Liv	Kariba	Middle Zambezi	25.82	-17.82	01/01/1998	31/12/2013	0.00	996
Senanga	Sen	Barotse	Upper Zambezi	23.27	-16.10	01/01/1998	31/12/2013	8.90	1001
Petauke	Pet	Luangwa	Middle Zambezi	31.28	-14.25	01/02/1998	31/12/2013	0.40	1006
Msekera	Msk	Luangwa	Middle Zambezi	32.57	-13.65	01/03/1998	31/12/2015	19.7	1028
	Kal	Lungue	Upper Zambezi						
Kalabo		Bungo		22.70	-14.85	01/01/1998	31/12/2011	5.20	1033
Mongu	Mong	Barotse	Upper Zambezi	23.15	-15.25	01/01/1998	31/12/2013	0.51	1052
Kasungu	Kas	Shire	Lower Zambezi	33.47	-13.02	01/01/2003	31/07/2013	0.00	1063
Victoria Falls	VF	Kariba	Middle Zambezi	25.85	-18.10	01/01/1998	31/12/2013	2.26	1065
Bolero	Bol	Luangwa	Middle Zambezi	33.78	-11.02	01/01/2003	31/05/2013	0.00	1070
	Za	Lungue	Upper Zambezi						
Zambezi		Bungo		23.12	-13.53	01/01/1998	31/12/2013	1.60	1075
Kabompo	Kap	Kabompo	Upper Zambezi	24.20	-13.60	01/01/1998	30/04/2005	0.08	1086
Chichiri	Chic	Shire	Lower Zambezi	35.05	-15.78	01/01/1998	31/12/2010	0.00	1136
Chitedze	Chtd	Shire	Lower Zambezi	33.63	-13.97	01/01/2003	30/04/2013	0.00	1150
Lundazi	Lu	Luangwa	Middle Zambezi	33.20	-12.28	01/01/2003	30/04/2013	1.40	1151
Guruve	Gur	Tete	Middle Zambezi	30.70	-16.65	01/01/1998	30/03/2013	0.02	1159
Kaoma	Kao	Barotse	Upper Zambezi	24.80	-14.80	01/01/1998	31/11/2013	9.89	1162
Bvumbwe	Bv	Shire	Lower Zambezi	35.07	-15.92	01/01/1998	01/01/2011	0.00	1172
Kasempa	Kas	Kafue	Middle Zambezi	25.85	-13.53	01/01/1998	31/12/2013	9.10	1185
Kabwe	Kab	Luangwa	Middle Zambezi	28.47	-14.45	01/01/1998	13/10/2012	1.54	1209
Chitipa	Chit	Shire	Lower Zambezi	33.27	-9.70	01/01/2003	06/01/2013	0.05	1288
Mwinilunga	Mwi	Kabompo	Upper Zambezi	24.43	-11.75	01/01/1998	31/12/2013	4.81	1319
Karoi	Kar	Tete	Middle Zambezi	29.62	-16.83	01/01/1998	31/12/2004	15.08	1345
Solwezi	Sol	Kafue	Middle Zambezi	26.38	-12.18	01/01/1998	31/12/2013	0.02	1372
Harare	HB	Tete	Middle Zambezi						
(Belvedere)				31.02	-17.83	01/01/1998	31/03/2013	7.80	1472
Harare(Kutsaga)	HK	Tete	Middle Zambezi	31.13	-17.92	01/01/2004	30/09/2010	0.55	1488
Mvurwi	Mv	Tete	Middle Zambezi	30.85	-17.03	01/01/1998	11/12/2000	0.00	1494
Dedza	Ded	Shire	Lower Zambezi	34.25	-14.32	01/01/2003	31/10/2012	0.00	1575

938
939

Table 2: Elevation zones influenced by correlation between the satellite and gauge based estimates.

Elevation zone	Station membership
< 250 m (lowland)	Marromeu, Caia, Nsanje, Makhanga, Nchalo, Ngabu, Chikwawa, Tete (Chingodzi)
250- 950 m (medium)	Chingodzi, Zumbo, Mushumbi, Kanyemba, Muzarabani, Monkey, Mangochi, Rukomechi, Mutarara, Mfuwe, Mimosa, Balaka, Thyolo, Chileka, Neno Mt Darwin, Chipata, Makoka, Livingstone, Senanga, Petauke, Msekekerera, Kalabo, Mongu,
> 950 m (highland)	Kasungu, Victoria Falls, Bolero, Zambezi, Kabompo, Chichiri, Chitedze, Lundazi, Guruve, Kaoma, Bvumbwe, Kasempa, Kabwe, Chitipa, Mwinilungu, Karoi, Solwezi, Harare (Belvedere), Harare (Kutsaga), Mvurwi, Dedza, Morrumbala

940
941

942
 943
 944
 945
 946
 947
 948
 949
 950
 951
 952
 953
 954
 955
 956
 957
 958
 959
 960
 961
 962
 963
 964
 965
 966
 967
 968
 969
 970

Table 3: Frequency based statistics for the CMORPH and gauge daily estimates for the lowland and highland stations in the Zambezi Basin

	Product type	Mean	St. dev	CV	max	sum	ratio
Lowland Stations	CMORPH	2.39	7.86	3.33	115.69	9796.81	
	Gauge	2.49	9.13	3.89	139.70	10486.42	0.93
Highland Stations	CMORPH	2.33	6.94	3.12	106.77	10099.85	
	Gauge	2.70	8.18	3.12	115.20	11578.93	0.87

971
 972
 973
 974
 975

976
 977
 978
 979
 980
 981
 982
 983
 984
 985
 986
 987
 988
 989
 990
 991
 992
 993
 994
 995
 996
 997
 998
 999
 1000
 1001
 1002
 1003
 1004
 1005

Table 4: Frequency based statistics for the gauge, uncorrected and bias corrected satellite rainfall for each of the Zambezi basins. Bold figures shows improved performance of the bias correction scheme from the uncorrected CMORPH when compared against the gauge based estimates

Basin	B-scheme	Mean	Std dev	Max	Sum	Ratio
Lower Zambezi	Gauge	2.62	9.17	142.77	10792.58	
	R-CMORPH	2.39	7.58	156.50	9540.65	0.88
	PT	2.12	8.42	139.33	8883.26	0.82
	QME	2.21	8.07	129.46	9349.42	0.87
	EZB	1.46	5.92	112.77	8529.38	0.79
	DT	2.00	7.78	137.53	11683.35	1.08
	STB	2.60	7.73	165.63	9494.89	0.88
Middle Zambezi	Gauge	2.47	8.33	109.81	10112.74	
	R-CMORPH	2.51	7.74	112.39	10373.64	1.03
	PT	1.93	6.55	109.76	9186.37	0.91
	QME	1.86	6.78	114.87	8150.50	0.99

	EZB	1.55	6.02	110.61	9039.03	0.89
	DT	1.81	6.73	115.79	10555.56	1.05
	STB	2.45	8.28	214.74	10488.24	1.04
Upper Zambezi	Gauge	2.55	7.82	117.24	13008.24	
	R-CMORPH	2.12	6.44	103.25	10722.09	0.82
	PT	1.94	5.83	90.52	10284.19	0.79
	QME	1.98	6.22	94.32	8674.54	0.67
	EZB	1.67	5.56	96.43	9750.19	0.75
	DT	2.49	7.72	112.81	14415.79	1.04
	STB	2.08	6.88	175.84	10850.88	0.83

1006

1007

1008

1009

1010

1011

1012

1013

1014

1015

1016

1017

1018

1019

1020

1021

1022

1023

1024

1025

1026

Table 5: Percentage of days that belong to the five rainfall intensities (0-2.5, 2.5-5, 5-10, 10-20 and >20 mm/day) for the Zambezi Basin. Bold figures shows best CMORPH performance when compared against the gauged and uncorrected CMORPH rainfall estimates.

	Rainfall intensity	Gauge	R_CMORPH	STB	PT	DT	EZB	QME
LZ	0.0-2.5	85.72	83.86	85.41	85.35	87.69	89.81	88.75
	2.5-5.0	2.87	4.71	4.30	4.20	3.08	2.80	3.09
	5.0 - 10	3.43	4.32	3.93	4.06	3.18	2.79	2.83
	10 - 20	3.53	3.78	3.38	3.48	2.88	2.39	2.45
	>20	4.45	3.32	2.98	2.91	3.17	2.20	2.88
MZ	0.0-2.5	84.91	83.67	87.38	86.38	88.55	90.24	83.74
	2.5-5.0	3.34	4.06	3.15	3.48	2.67	2.40	2.75
	5.0 - 10	3.90	4.31	3.42	3.75	3.02	2.41	2.79
	10 - 20	3.89	4.05	3.02	3.45	2.88	2.55	2.63
	>20	3.96	3.92	3.03	2.95	2.89	2.40	9.00
UZ	0.0-2.5	84.14	82.01	83.77	83.68	83.36	80.34	84.91
	2.5-5.0	3.62	5.30	5.01	5.08	4.35	5.50	3.29

5.0 - 10	4.24	5.62	5.01	5.11	4.80	5.76	3.27
10 - 20	4.09	4.35	3.76	3.87	4.19	5.07	2.77
>20	3.91	2.73	2.45	2.25	3.30	3.32	5.75

1027
1028
1029
1030
1031
1032
1033
1034
1035
1036
1037
1038
1039
1040
1041
1042
1043
1044
1045
1046
1047
1048
1049
1050
1051
1052
1053

Table 6: Frequency based statistics for the gauge, uncorrected and bias corrected satellite rainfall for the dry and wet seasons.

Basin	Bfactor	Dry season					Wet season				
		Mean	Std dev	Max	Sum	Ratio	Mean	Std dev	Max	Sum	Ratio
LZ	Gauge	0.46	2.78	60.9	908.60		4.89	12.60	143.2	10039.9	
	R-CMORPH	0.39	2.42	55.4	836.47	0.92	4.29	9.91	110.5	8616.7	0.86
	PT	0.32	2.12	48.7	706.46	0.78	3.64	10.46	121.5	7563.1	0.75
	DT	0.22	2.60	65.9	654.12	0.72	3.64	9.94	109.0	10612.2	1.06
	QME	0.27	2.03	57.7	792.95	0.87	2.60	7.79	109.9	7564.8	0.75
	EZB	0.27	2.05	59.1	793.63	0.87	2.65	7.92	112.4	7729.0	0.77

	STB	0.37	2.39	56.3	866.58	0.95	3.93	10.19	117.3	8612.7	0.86
MZ	Gauge	0.33	4.69	187.9	762.88		4.99	18.31	238.1	10681.5	
	R-CMORPH	0.19	1.84	46.2	393.98	0.52	4.73	10.18	110.7	9969.2	0.93
	PT	0.13	1.41	38.1	319.72	0.42	3.27	7.85	163.5	7993.3	0.75
	DT	0.31	2.52	61.6	921.73	1.21	6.52	13.47	97.4	19032.2	1.78
	QME	0.13	1.52	45.8	370.56	0.49	2.97	8.10	108.3	8638.9	0.81
	EZB	0.13	1.51	45.6	369.73	0.48	3.00	8.11	108.3	8740.8	0.82
	STB	0.15	1.63	46.6	381.09	0.50	3.96	11.12	100.9	10187.7	0.95
UZ	Gauge	0.24	2.53	70.4	640.40		5.57	11.04	120.6	13240.4	
	R-CMORPH	0.22	1.98	61.1	577.44	0.90	4.56	8.75	101.4	10700.6	0.81
	PT	0.20	1.80	54.3	513.02	0.80	3.52	7.01	112.6	9130.1	0.69
	DT	0.08	2.12	64.8	233.24	0.36	3.48	7.83	105.0	10146.7	0.77
	QME	0.18	1.81	58.9	524.21	0.82	3.10	7.20	97.8	9022.3	0.68
	EZB	0.18	1.85	59.3	534.50	0.83	3.15	7.13	97.2	9199.9	0.69
	STB	0.23	2.11	63.1	601.79	0.94	3.97	8.91	112.8	10127.4	0.76

1054
1055
1056
1057
1058
1059
1060
1061
1062
1063
1064

Table 7. Performance of uncorrected CMORPH (R-CMORPH), and the bias corrected CMORPH's Elevation zone bias (EZB) for three stations in the Middle Zambezi valley (Mushumbi, Kanyemba and Zumbo) and three on the escarpment (Guruve, Karoi and Mvurwi)

		Mushumbi	Kanyemba	Zumbo	Guruve	Karoi	Mvurwi
ELEVATION (m)		369	372	345	1159	1345	1494
Bias	R-CMORPH	-0.10	-0.33	-0.17	-0.05	0.03	0.53
	EZB	0.08	-0.07	0.001	0.27	0.35	0.8
Rbias	R-CMORPH	-5.38	-13.57	-8.35	-1.97	1.07	20.61
	EZB	0.21	4.22	10.22	13.63	25.98	4.22
RMSE	R-CMORPH	7.04	9.16	7.62	7.49	7.32	9.88
	EZB	7.44	9.56	8.06	7.43	7.44	9.99
CC	R-CMORPH	0.62	0.42	0.53	0.52	0.51	0.32
	EZB	0.55	0.36	0.50	0.49	0.47	0.28

1065